

1 Marine submicron aerosol sources, sinks and 2 chemical fluxes

3
4 **D. Ceburnis¹, M. Rinaldi², J. Keane-Brennan¹, J. Ovadnevaite¹, G.
5 Martucci¹, L. Giulianelli², C.D. O'Dowd¹**

6 [1]School of Physics and Centre for Climate & Air Pollution Studies, Ryan
7 Institute, National University of Ireland, Galway, University Road, Galway,
8 Ireland

9 [2]Institute of Atmospheric Sciences and Climate, National Research Council,
10 Bologna, Italy

11 Correspondence to: D. Ceburnis (darius.ceburnis@nuigalway.ie)

12 13 **Abstract**

14 Aerosol physico-chemical fluxes over NE Atlantic waters were quantified
15 through the parallel deployment of micrometeorological eddy covariance flux
16 system and an aerosol chemistry gradient sampling system. Fluxes of primary
17 components, specifically, sea salt, water insoluble organic carbon (WIOC) and a
18 combined sea spray and secondary aerosol components, specifically, nitrate,
19 ammonium, oxalate, amines, methanesulfonic acid (MSA) and water soluble
20 organic nitrogen (WSON) are presented in the context of seasonality of marine
21 aerosol sources and sinks. A strong power law relationship between fluxes and
22 wind speed has been obtained for primary sea salt and sea spray while water
23 insoluble organic matter (WIOM) followed a linear dependency. The power law
24 relationship between sea salt flux (F_{SS}) and 10m height wind speed (U_{10})
25 ($F_{SS}=0.0011U_{10}^{3.15}$) compared very well with existing parameterisations but
26 highlighted the divide between parameterization derived from ambient
27 observation versus laboratory measurements. The observed seasonal pattern of
28 sea salt production was mainly driven by wind action with the tentative effect of
29 marine OM. WIOM wind dependent fluxes were a complex combination of
30 rising and waning biological activity, especially in the flux footprint area, and
31 wind-driven primary sea spray production supporting the coupling of recently
32 developed sea spray and marine OM parameterisations.

33

34 **1. Introduction**

35 Marine aerosols contribute significantly to the global radiative budget and
36 consequently, changes in marine aerosol abundance and/or chemical composition
37 have an impact on climate change through both direct and indirect effects. The
38 Northeast Atlantic region is of particular interest due to a combination of
39 storminess, prevailing westerlies bringing marine air masses into continental
40 Europe, and biological activity in surface waters significantly affecting chemical
41 composition of atmospheric particulate matter (O'Dowd et al., 2004). Organic
42 matter (OM) has been observed in marine aerosol particles for many decades and
43 has been linked to fractional contribution of OM transferred from the sea-surface
44 into the tropospheric boundary layer through bubble-mediated production
45 processes (Blanchard, 1964; Hoffman and Duce, 1977; Middlebrook et al., 1998;
46 Oppo et al., 1999; Russell et al., 2010). There has been a significant progress in
47 understanding marine aerosol composition, which has been identified to consist
48 of significant amounts of organic matter (Cavalli et al., 2004; Sciare et al., 2009)
49 both water-soluble and water-insoluble. It has historically progressed from
50 mainly consisting of sea salt and non-sea salt sulphate (Charlson et al., 1987;
51 O'Dowd et al., 1997) to complex primary biogenic organic mixtures and states
52 (dissolved, particulate, colloidal or nanogel) (Cavalli et al., 2004; Leck and Bigg,
53 2005; Russell et al., 2010; Decesari et al., 2011) as well as secondary organic
54 compounds like organic acids (Kawamura and Sakaguchi, 1999; Mochida et al.,
55 2002; Turekian et al., 2003; Rinaldi et al., 2011) and recently discovered
56 biogenic amines (Facchini et al., 2008a; Muller et al., 2009). The findings of
57 Ceburnis et al. (2008) and Facchini et al. (2008b) independently confirmed that
58 water insoluble organic carbon (WIOC) in marine atmosphere has primary origin
59 while water soluble organic carbon (WSOC) is mainly secondary or processed
60 primary (Decesari et al., 2011), however, studies of Keene et al. (2007) and
61 Russell et al. (2010) evidenced that even WSOC can largely be of primary origin.
62 After significant fraction of marine sea spray particles was found to contain
63 biogenic organic matter compounds (O'Dowd et al., 2004) it became even more
64 important to determine principal sources and sinks of marine organic matter.
65 Tentatively, the source of biogenic marine organic matter has been linked to the
66 ocean surface and driven by a biological activity in surface waters based on a
67 seasonality pattern of organic matter and chlorophyll-a (Yoon et al., 2007; Sciare

68 et al., 2009) or regression analysis (O'Dowd et al., 2008; Russell et al., 2010).
69 Furthermore, the first quantitative estimate of submicron aerosol organic matter
70 in oceanic environment has been performed by Ceburnis et al. (2011) using dual
71 carbon isotope analysis that showed over 80% of organic matter in clean marine
72 air masses is of marine biogenic origin. A pilot study based on concentration
73 gradient method performed in marine environment by Ceburnis et al. (2008)
74 revealed that water soluble organic matter is largely produced by secondary
75 processes while water insoluble organic matter is of primary origin. The latter
76 study evaluated the first wind speed dependent fluxes, but those remained
77 uncertain due to the absence of parallel eddy covariance measurements and a
78 limited sampling period. Considering a significant seasonal cycle of marine
79 organic matter is important to study chemical fluxes on a full year basis to
80 capture the variability in aerosol sources and sinks.

81 This study is the extension of the study by Ceburnis et al. (2008) through the
82 combination of eddy covariance measurements in parallel with the off-line
83 chemical analysis of samples, expansion of the range of chemical species and
84 extension of the timescale to evaluate fluxes as a function of season.

85

86 **2. Experimental methods**

87 The flux of sea-spray aerosols has been studied previously as sea salt mass fluxes
88 or aerosol size and number flux (O'Dowd and De Leeuw, 2007; de Leeuw et al.,
89 2011). Apart from few studies, the flux experiments have typically focused on
90 super-micron sized particles. Eddy covariance method for studying submicron
91 particle fluxes was first used by Buzorius et al. (1998) estimating submicron
92 particle fluxes and sinks and has been since applied in a variety of environments:
93 boreal and tropical forest (Buzorius et al., 1998; Ahlm et al., 2009), ocean
94 (Nilsson et al., 2001; Geever et al., 2005; Norris et al., 2008; Brooks et al., 2009),
95 desert (Fratini et al., 2007) and urban (Martensson et al., 2006; Martin et al.,
96 2009). Eddy-covariance method is typically used to study total particles fluxes.
97 The technique has been modified into relaxed eddy-covariance method to allow
98 studying size-segregated particle fluxes (Gaman et al., 2004) or disjunct eddy
99 covariance method (Held et al., 2007) employing slower response instruments. It
100 should be noted, however, that while number of sea spray particles is dominated
101 by submicron particles, mass is dominated by super-micron sizes and not a single

102 method is capable of measuring particles around the important boundary of 1
103 micrometer. None of the above techniques were suitable for studying chemically
104 resolved fluxes, because chemical analysis typically requires long sampling time
105 (many hours for off-line chemical analysis). Most recently, however, eddy-
106 covariance system coupled with high resolution aerosol mass spectrometer has
107 been used to study chemically resolved fluxes (Nemitz et al., 2008; Farmer et al.,
108 2011), but those were largely limited to areas with relatively high concentration
109 of species.

110 The study of chemical fluxes in a relatively clean marine atmosphere represents a
111 great challenge due to generally low absolute species concentrations and the lack
112 of appropriate experimental methods. The rationale of choosing the gradient-flux
113 method was based on the fact that persistent fluxes must produce concentration
114 gradients with their sign depending on the source and assuming that recurrent
115 eddies allow sampling for certain number of hours to meet analytical
116 requirements of chemical species. Additional challenges exist when it comes to
117 reactive species (organic matter) due to chemical transformation during transport
118 to the sampling location or extended sampling durations. A combination of
119 continuous production (or removal) of particles and turbulent eddies of varying
120 magnitude within the boundary layer should establish concentration profiles. The
121 profiles, therefore, are a net result of the competition between upward and
122 downward eddies averaged over time. The persistent surface source will manifest
123 itself in a decreasing concentration away from the source. The absence of the
124 surface source should result in an increasing concentration profile as particles are
125 removed to the surface through deposition processes. For the approach to work
126 one needs neutral or near-neutral boundary layer stability conditions persisting
127 for sufficient timescales to allow sampling over many hours. The biggest caveat
128 is whether representative averaging over many hours can produce meaningful
129 results. The approach was previously demonstrated to work in urban
130 environment (Valiulis et al., 2002) as well as in a relatively clean marine
131 environment (Ceburnis et al., 2008). This study is the continuation of the latter
132 study adding full scale eddy-covariance system and expanding the number of
133 chemical species studied.

134 A new set-up to study gradient chemical fluxes was installed at Mace Head
135 Atmospheric Research Station on the west coast of Ireland (Jennings et al., 2003;

136 O'Connor et al., 2008) comprising PM1 samplers installed at three different
137 heights (3 m, 10 m, and 30 m) while the eddy covariance system installed at the
138 22 meter height.

139 LIDAR measurements (Jenoptik/Lufft and Vaisala ceilometers) are continuously
140 conducted at Mace Head and a dedicated algorithm for temporal height tracking
141 (THT) (Haeffelin et al., 2012; Milroy et al., 2012) using the backscatter profiles
142 measured by the LIDAR was used to identify the surface mixed layers (SML)
143 and the decoupled residual layers (DRL), both important parameters when
144 considering boundary layer filled by primary fluxes.

145 The chlorophyll satellite data (daily, 1° spatial resolution) were obtained from
146 GlobColour (<http://www.globcolour.info>). They result from the merging of
147 Medium-Resolution Imaging Spectrometer (MERIS), Moderate Resolution
148 Imaging Spectroradiometer (MODIS), and Sea-viewing Wide Field-of-view
149 Sensor (SeaWiFS) data, using advanced retrieval based on fitting an in-water
150 biooptical model to the merged set of observed normalized water-leaving
151 radiances. A thorough description of the data treatment can be found in Rinaldi et
152 al.(2013).

153

154 **2.1 Sampling strategy**

155 Meteorological records demonstrate that on average marine westerly air masses
156 account for over 50% of time at the station (Cooke et al., 1997; Jennings et al.,
157 2003). The gradient measurement system PM1 samplers (Sven Leckel
158 Ingenieurbüro GmbH) ran in parallel at a flow rate of 38 lpm. Samples were
159 collected in clean marine conditions (wind direction $190 < WD < 300$ and
160 Condensation Particle Counter (CPC) concentrations < 700 particles cm^{-3}) using
161 an automated sampling system on quartz filters for the analysis of both organic
162 and inorganic components of marine aerosol. The system operated day and night
163 whenever the above clean marine conditions were met. Active control of the
164 sampling conditions excluded sampling during occasional short-term spikes of
165 CPC concentrations either due to coastal nucleation events or occasional local
166 ship traffic. Post-sampling analysis revealed that such air masses did not have
167 contact with land for 4-5 days (as confirmed by air mass back-trajectories) and
168 black carbon (BC) concentration measured by an Aethalometer (AE-16, Magee
169 Scientific, single wavelength at 880 nm) did not exceed 50 ng m^{-3} . Such air

170 masses have been typically spending the last 48 hours (at least) in the marine
171 boundary layer as documented by Cavalli et al. (2004) and Ceburnis et al. (2011).
172 The latter study quantitatively demonstrated that in clean marine air masses
173 anthropogenic carbon species typically contributed to 8-20% of the total carbon
174 mass which should be applicable to other anthropogenic species due to internally
175 mixed anthropogenic aerosol far from the source. It is important to note that
176 clean marine samples collected at Mace Head are representative of the open
177 ocean environment considering chemical and physical similarities between open
178 ocean and coastal (Mace Head) samples (Rinaldi et al., 2009). The marine air
179 criteria used at Mace Head were demonstrated to be sufficient at ensuring that
180 anthropogenic and coastal effects are minimised to guarantee a dominant, if not
181 at times overwhelming natural marine aerosol signal as detailed in the study of
182 O'Dowd et al.(2014).

183

184 **2.2 Off-line chemical analysis and concentration gradients**

185 Fifteen PM1 gradient samples were collected during 13 month period in clean
186 marine conditions as listed in Table 1. The sampling strategy aimed at capturing
187 two samples per month providing that clean marine conditions were prevailing
188 and each sample duration lasted on average 50% of time during the calendar
189 week.

190 The samples were analysed for a wide range of chemical species present in
191 aerosol particles: sodium (a marker for sea salt (SS)), non-sea-salt sulphate
192 (nssSO_4), nitrate (NO_3), ammonium (NH_4), methanesulphonic acid (MSA), total
193 carbon (TC), oxalate (Oxa), (analytical details can be found in Cavalli et al.
194 (2004)), water soluble organic carbon (WSOC), water insoluble organic carbon
195 (WIOC) (Rinaldi et al., 2009), water soluble organic nitrogen (WSON), total
196 nitrogen (TN), dimethylamine (DMA) and diethylamine (DEA) (Facchini et al.,
197 2008a). WIOC was calculated as $\text{WIOC}=\text{TC}-\text{WSOC}$ while WSON was
198 calculated as $\text{WSON}=\text{TN}-\text{WSIN}$ (water soluble inorganic nitrogen). WSOM
199 (water soluble organic matter) was calculated as $\text{WSOC}*1.8$ and WIOM (water
200 insoluble organic matter) was calculated as $\text{WIOC}*1.4$ (Decesari et al., 2007;
201 Facchini et al., 2008b). Sea salt concentration was calculated as $\text{SS}=\text{Na}*3.1$
202 (Seinfeld and Pandis, 2006). The absolute concentration ranges of all measured
203 components are summarised in Table 2.

204 Concentration gradients of various chemical species were obtained by linear fit
205 of the concentration profile (except WSOM). A detailed discussion of potential
206 influence of local sources (surf-zone) to the gradient can be found in (Ceburnis et
207 al., 2008) and reconsidered in the Results section. Normalised averaged
208 concentration profiles of all measured chemical species were obtained as follows:
209 for each aerosol component, only samples for which concentrations above the
210 detection limit were observed at all three sampling altitudes were used in data
211 analysis. Normalisation was done by dividing the concentration at every height
212 by the sum concentration of three levels thus giving the same weight to every
213 profile for averaging purposes. After normalisation, the profiles of each mass
214 category were averaged, resulting in statistically meaningful variances around the
215 mean value and presented as an average and its standard deviation. The main
216 features were similar to the ones documented by (Ceburnis et al., 2008):
217 decreasing concentration with height, or negative gradient, was common of
218 species produced at the surface by primary processes while increasing
219 concentration with height, or positive gradient, was common of species produced
220 by secondary processes in the atmosphere aloft or within the marine boundary
221 layer.

222

223 **2.3 Eddy-covariance system**

224 Eddy-covariance measurements of micrometeorological parameters, water
225 vapour (H₂O) and CO₂ fluxes were undertaken in parallel (Keane-Brennan,
226 2011) which provided micrometeorological measurement data for calculating
227 gradient fluxes. The flux package comprised a Solent sonic anemometer (Gill
228 Windmaster Pro) to provide 3-D wind fields at 10 Hz. The sonic anemometer
229 was mounted 2 meters out from the sea-facing side of the 22 m tower and a
230 turbulent flow around the tower (Buzorius et al., 1998). Flux data were averaged
231 for 30 min for further analysis and more details on flux data can be found in
232 Geever et al. (2005) and Keane-Brennan et al. (2011). Half-hourly flux data were
233 further averaged to match the periods of gradient samples. The undertaken
234 strategies allowed a complete analysis of the source and sink fluxes as a function
235 of wind speed and oceanic biological activity and provided a quantification of
236 both primary and secondary inorganic and organic aerosol species cycling in the
237 marine boundary layer.

238

239 **2.4 Flux-gradient method**

240 First-order closure turbulent flux parameterisation, often known as a gradient
241 transport theory, K -theory or flux-gradient similarity method, can be expressed
242 according to Stull (1988) as following:

243

$$244 \quad F = -K_z \left. \frac{dc}{dz} \right|_z \quad (1)$$

245 where F is the flux, K_z is the turbulent-transfer coefficient; dc/dz is the
246 concentration gradient.

247

248 Thus having K_z value and the measured concentration gradient it is possible to
249 calculate fluxes of chemical species. The approach, however, would only allow
250 calculating the net flux and does not allow distinguishing between upward and
251 downward fluxes in high time resolution as is typically done with the eddy
252 covariance system. The K_z parameter can be calculated from the eddy covariance
253 (EC) measurements using high frequency data of vertical wind velocity using the
254 formula: $\sigma = \sqrt{2K_z t}$ (where σ is the standard deviation of vertical wind velocity, K_z
255 is the turbulent-transfer coefficient, t is time). K_z had to be averaged over about
256 50 to 140 hours to represent the sampling period of a particular concentration
257 profile. The averaged K_z values were compared with eddy covariance data and
258 presented in Figure 1 to check whether the averaged K_z values were consistent
259 with the high time resolution measurements. The dependence of K_z values on
260 horizontal wind speed were very similar pointing to the fact that K_z values were
261 consistently distributed around the mean and the mean average representing
262 gradient samples was statistically meaningful. The variance of K_z values around
263 the mean provided the partial uncertainty in flux calculations. It is worth noting
264 that the power law coefficient of the averaged K_z (WS) dependence was very
265 similar to the one given by Ceburnis et al. (2008) (1.97 and 2.07 respectively). A
266 similarity between the relationships obtained by Ceburnis et al. (2008) from 2002
267 EC data and this study period (2008-2009) suggests that the dynamics of the
268 boundary layer did not change significantly over time at this geographical
269 location, thereby providing a confidence that the K_z values can be reliably
270 derived from the horizontal wind speed measurements if the K_z values cannot be

271 estimated directly. However, the above relationship between horizontal wind
272 speed and the coefficient of turbulent transfer would only apply to the marine
273 sector and Mace Head location. The scatter of K_z values over a short or long
274 period of time was mainly due to gustiness as presented in Figure 2 where the K_z
275 and wind speed relationship was coloured by normalised standard deviation of
276 the horizontal wind using random subset of data. All elevated values of K_z were
277 accompanied by high values of the standard deviation of the horizontal wind
278 speed. Therefore, K_z values were all meaningful and must have been included in
279 the mean average to represent fast turbulent eddies.

280 It is important to know the thickness of the surface layer as it is here that fluxes
281 are considered to be constant and gradients adhere to similarity theory. Another
282 caveat is the formation of internal boundary layers (Stull, 1988). Detailed
283 measurements performed during NAMBLEX campaign at Mace Head (Heard et
284 al., 2006) provided strong evidence that the internal boundary layer had little
285 impact on the measurements made on the main tower if they were conducted
286 above 7-10 m (Coe et al., 2006; Norton et al., 2006), which would include two
287 out of our three sampling points. Norton et al. (2006) showed that the internal
288 boundary layer was typically limited to below 10m and never propagated to the
289 top of the tower in marine sector. Coe et al. (2006) concluded that over a wide
290 range of aerosol sizes there was no impact of the inter-tidal zone or the surf zone
291 on measurements made at 7m above ground level or higher.

292

293 **2.5 Errors and uncertainties**

294 The flux-gradient method based on the Equation 1, involves several variables,
295 necessitating a calculation of the combined propagated uncertainty. Specifically,
296 not only it involved two independently measured concentrations at two heights,
297 but the uncertainty of the subtracted blank concentration (pre-fired but not
298 exposed filter) and the uncertainty of the K_z value. The combined fractional
299 uncertainty of an individual flux was calculated by the following Equation:

300

$$301 \quad \delta q = \sqrt{\left(\frac{\partial q}{\partial x_1} \delta x_1\right)^2 + \dots + \left(\frac{\partial q}{\partial x_n} \delta x_n\right)^2} \quad (2)$$

302 where x_i are the independent variables and δx_i are the fractional uncertainties of
303 the independent variables.

304 The uncertainty of individual concentrations (C) and the gradient (G) was
305 calculated by the following Equation:

$$306 \quad \delta C = \sqrt{(\delta C_{meas})^2 + (\delta C_{blank})^2} \quad (3)$$

$$307 \quad \delta G = \sqrt{(\delta C_{10})^2 + (\delta C_{30})^2} \quad (4)$$

308 where C_{meas} , C_{blank} , C_{10} and C_{30} were measured, blank and concentration at 10
309 and 30 meters, respectively.

310 The relative uncertainty of the corresponding fluxes was calculated by the
311 following Equation based on multiplication of measured quantities ($F=G*K_z$):

$$312 \quad \frac{\delta F}{F} = \sqrt{\left(\frac{\delta G}{G}\right)^2 + \left(\frac{\delta K_z}{K_z}\right)^2} \quad (5)$$

313 where G and K_z are corresponding gradients and coefficient of turbulent transfer,
314 respectively. Note that the flux uncertainty is dominated by the gradient
315 uncertainty, because the uncertainty of turbulent transfer coefficient would be
316 actually smaller than presented in Eq. 5 due to being an average of over a
317 hundred of half-hourly values.

318 The relative uncertainty of the organic matter fractional contribution to sea spray
319 ($OM_{ss}=WIOM/(WIOM+SS)$), where the variable $WIOM$ appeared in both
320 nominator and denominator and $WIOM$ represented total sea spray OM, resulted
321 in a more complicated equation of the combined propagated uncertainty of the
322 OM fractional contribution:

$$323 \quad \frac{\delta OM_{ss}}{OM_{ss}} = \frac{SS}{(SS+WIOM)} \sqrt{\left(\frac{\partial WIOM}{WIOM}\right)^2 + \left(\frac{\partial SS}{SS}\right)^2} \quad (6)$$

324 where the ratio in front of the square root is the fractional contribution of sea salt
325 in sea spray resulting in the fractional uncertainty of the OM fractional
326 contribution dependent on the sea salt fractional contribution and, therefore,
327 always smaller than the additively combined fractional uncertainty of sea salt and
328 WIOM measurement.

329 The uncertainty of the fitted functional relationships obtained from the discretely
330 measured values was presented with the 95% confidence bands which was
331 conceptually different from the fractional uncertainties of individual values. The
332 confidence bands also helped to define the best fitted function (e.g. linear or
333 power law) as unrealistic fits had very low or no confidence at all. Typically, the
334 confidence bands become narrower as the number of points increases and/or their
335 scatter decreases. The presentation of the confidence bands provided the physical

336 meaning of the points residing outside the confidence bands. An individual point
337 which is outside the confidence bands suggests a higher order of the relationship
338 or an unaccounted freak error. Several of such cases will be discussed
339 accordingly.

340

341 **3 Results and Discussions**

342 The measurements at three different heights allow resolving the vertical
343 concentration profiles of different chemical species and the magnitude of the
344 sources and sinks, or corresponding fluxes, shape the profiles. Most of them were
345 non-linear, but well interpretable having studied concentration and flux footprints
346 in detail in the previous pilot study of (Ceburnis et al., 2008). It is important to
347 note that the footprint of the measured absolute concentration was of many tens
348 to hundreds of kilometres offshore while the footprint of the concentration
349 gradient or the flux was within about 10km from the measurement location, i.e.
350 coastal waters (Ceburnis et al., 2008). The surf zone emissions may have had
351 certain influence on the concentrations of sea salt or sea-spray at the lowest level
352 of 3m, particularly for low wind speeds, practically disappearing at higher
353 winds(O'Dowd et al., 2014), but had little or no impact on secondary organic
354 aerosol. The different distances of the flux footprint arise from emissions
355 contributing to the concentration at different heights. The flux footprint of the
356 90% concentration difference between 3 and 10 meters is 0.2-1.2 km while the
357 footprint of the 90% of the difference between 10 and 30 meters extends to 5 km
358 (Figure 1, Ceburnis et al. 2008). The remaining 10% of the contribution extends
359 well beyond 5km, perhaps 10 km distance being a safe approximation. A
360 condensation potential could have also contributed to the concentration
361 differences of certain species as the time required for the air parcel to cover 10
362 km distance is about 15 min which is more than sufficient to achieve gas-aerosol
363 equilibrium, e.g. (Meng and Seinfeld, 1996; O'Dowd et al., 2000).

364

365 **3.1 Concentration gradient profiles**

366

367 **3.1.1 Primary components**

368 The concentration profile of sea salt (top left in Figure 3) was unambiguously
369 surface sourced or primary, i.e. concentration was decreasing vertically. Some of

370 the individual profiles were sharper than others, but all were primary with only
371 three exceptions where the profiles were distorted at lower heights possibly
372 partly due to measurement errors and partly due to boundary layer dynamics and
373 changes in sea state during the sampling period (ascending and descending wind
374 regimes). However, as it was stated above, surf-zone emissions could have had
375 influenced the concentration value at the lowest level of 3 meters and, therefore,
376 this level was not used in the flux calculations of primary sea spray species.

377 Interestingly, similar “negative gradient” concentration profiles were obtained
378 for nitrate and oxalate. However, those profiles were slightly, but systematically
379 distorted, i.e. the concentrations of oxalate and nitrate significantly diverged
380 from the sea salt one at the lowest sampling height of 3 meters while following
381 the sea salt profile above 10 meters. It is well established that nitrate is produced
382 by secondary processes and mainly manifesting itself through condensed nitric
383 acid on pre-existing sea salt particles in the absence of anthropogenic ammonium
384 nitrate. Sea salt particles at the lowest level were the freshest having the closest
385 flux footprint and, consequently, adsorbed the least amount of condensable nitric
386 or oxalic acid compared to higher levels. Similarly to nitrate, oxalic acid could
387 have been condensing on pre-existing sea salt particles as well despite more
388 diverse chemical pathways of oxalic acid (some of the oxalate could also be
389 produced by oxidation of organic matter inside sea-spray particles (Rinaldi et al.,
390 2011) and, therefore, manifesting itself as “primary” species. The concentration
391 profile of oxalic acid was similar to that of nitrate and could indicate that a
392 significant amount of oxalate is produced in the atmosphere aloft subsequently
393 condensing onto primary sea spray particles due to its acidic nature.

394 The water insoluble organic matter (WIOM) concentration profiles were split
395 between three main categories: production (5 profiles), removal (6 profiles) and
396 mixed profiles (4 profiles) (bottom right of Figure 3). Given that fractional
397 contribution of OM in primary sea spray is related to the enrichment of organic
398 matter at the ocean surface, this range of behaviour can be interpreted in terms of
399 the location of biologically active region relative to the flux footprint. The
400 biologically active water patches within the flux footprint (~10 km from the
401 measurement location) were responsible whether WIOM was produced or
402 removed from the surface layer, or a combination of both processes. Therefore, a
403 mixed profile was pointing at the production at a longer distance from the coast

404 and the removal close to the measurement location. Thus the removal profile was
405 pointing both at the deposition within the flux footprint area and/or the absence
406 of biological activity in surface waters within the flux footprint area. The WIOM
407 production by the secondary processes cannot be completely excluded either, but
408 we have no evidence of that. It is worth noting that the production profiles were
409 observed in early spring (March until early May) when biological activity is high
410 at the coast and during late summer (late July-August) when biological activity
411 has a second maximum identified by the chlorophyll proxy (Yoon et al., 2007).
412 In contrast, the removal profile was observed during late spring and early
413 summer when biological activity is retreating away from the coast into the open
414 ocean. Despite a general pattern of the evolution of biological activity presented
415 by Yoon et al. (2007) it should be stressed that biological activity is very patchy
416 all over the ocean including coastal areas and the phytoplankton blooms are
417 generally governed by the availability of nutrients which themselves are supplied
418 by ocean currents and upwelling and become unpredictable on a day-to-week
419 time scale.

420

421 **3.1.2 Secondary components**

422 The inorganic secondary species (nssSO_4 and NH_4) are presented in top right of
423 Figure 3 along with an aerosol neutralisation profile considering only ammonium
424 and sulphate which will be discussed later. Ammonium profile was clearly
425 secondary, as expected, due to ammonia being the principal gaseous neutralizing
426 agent in the marine boundary layer. It should be noted that the concentration
427 profile of nssSO_4 was pretty constant and did not follow that of the ammonium
428 profile as it could be expected considering that sulphuric acid is the main acidic
429 species in the marine boundary layer, typically neutralized by ammonium.
430 NssSO_4 was calculated as the difference between two relatively large numbers
431 (total measured SO_4 minus sea-salt SO_4 as inferred from a conservative tracer
432 such as Na ion). As sea salt concentration was changing quite dramatically with
433 height especially in moderate to high wind speed during winter, some ambiguity
434 must be acknowledged before interpreting nssSO_4 profile. In fact, if the winter
435 sulphate profiles were excluded from the average that would have improved the
436 average profile. In any event nssSO_4 concentrations at three different heights
437 were not significantly different preventing any conclusions with respect to

438 apparently secondary nssSO₄. The uncertainty in nss-sulphate determination can
439 be the reason of the difference with respect to the profile of ammonium. Looking
440 at the profiles, it can be observed that marine aerosol sampled at Mace Head is
441 more neutralized at 30 m than closer to the sea level (Figure 3 (top right) and
442 Figure 4), even though neutralization with respect to sulphuric acid is never
443 complete, due to scarcity of ammonia in the marine boundary layer. Figure 4
444 shows calculated ammonium (considering full neutralisation) versus measured
445 ammonium revealing significant but consistent differences in neutralisation
446 pattern at three different heights. The neutralization profile can be driven by the
447 gaseous ammonia vertical profile, which we have no hint about, or can be an
448 indication of the importance of in-cloud processes of sulphate neutralization
449 considering also that measurements at the lowest level were somewhat perturbed
450 due to surf-zone fluxes. In fact, if the neutralization of acidic sulphates occurred
451 prevalently in clouds, after scavenging of gaseous ammonia into acidic droplets,
452 this process would occur more likely at the top of the marine boundary layer,
453 were cloud layers form, justifying the observed neutralization profile.

454 The secondary organic species (MSA, WSOM and WSON) are presented in the
455 bottom left of Figure 3. The MSA exhibited a “mixed profile” with steep increase
456 of concentration between 3 and 10 m, typical of secondary products and
457 decreasing profile between 10 and 30 m, likely due to condensation of MSA on
458 sea salt particles (Hopkins et al., 2008) that causes an apparently primary profile.
459 A clear secondary profile was observed for WSOM also, reaffirming the
460 conclusion of Ceburnis et al. (2008) on the secondary origin of WSOM. The
461 water soluble organic nitrogen concentration pattern is presented in the bottom
462 left of Figure 3. WSON presents a mixed profile, therefore, it is not possible to
463 attribute it to primary or secondary formation processes unambiguously. WSON
464 concentration in aerosol samples is generally difficult to quantify as it is
465 calculated as the difference between the total nitrogen (TN) and the water soluble
466 inorganic nitrogen (WSIN) – both numbers of similar magnitude. As a result,
467 only 7 complete profiles could be derived out of 15 samples and should,
468 therefore, be considered cautiously (8 profiles were discarded as incomplete, i.e.
469 missing determined concentration at one or two levels). Along with WSON,
470 aliphatic amines were analysed following Facchini et al. (2008a). WSON, DMA
471 and DEA are minor constituents of marine aerosol, together typically accounting

472 for 10% of secondary organic aerosol (Facchini et al., 2008a). While the
473 magnitude of their absolute concentrations may be misleading – amines can be
474 important species facilitating new particle production in the marine atmosphere
475 (Dall'Osto et al., 2012) – quantification of their concentration by offline chemical
476 analysis is always challenging. Mostly concentrations of DMA and DEA at the
477 lowest height were below detection limit and, therefore, no profile can be
478 provided for these species with confidence. However, the fact that detectable
479 concentrations were always observed at 30 m, strongly suggests a secondary
480 origin for DMA and DEA.

481 The well-established aerosol chemical compounds such as nitrate, oxalate, MSA
482 and less well established WSON were all studied for the first time using flux-
483 gradient method. The concentration profiles of the above compounds have not
484 demonstrated that the species were secondary, despite well-established
485 knowledge of their secondary formation in the atmosphere aloft (boundary layer,
486 clouds or free troposphere)(Seinfeld and Pandis, 2006; Facchini et al., 2008a;
487 Rinaldi et al., 2011). Figure 5 is presented for elucidating an apparent “primary”
488 profile of nitrate and oxalate which is due to aforementioned species condensing
489 or reacting with sea spray particles. MSA by contrast has the weakest if any
490 relationship with sea salt. Figure 5 (top left) presents the relationship between
491 nitrate and sea salt mass which appears as linear with the exception of 2-3
492 outliers. The outliers likely appeared due to the presence of trace amounts of
493 ammonium nitrate. Ammonium nitrate is generally considered as anthropogenic
494 species and can be present in trace amounts due to pollution background. The
495 trace amount was really small, 20-30 ng m⁻³ of nitrate only re-affirming
496 cleanness of the marine atmosphere studied at Mace Head. Despite a strong
497 similarity in concentration pattern of nitrate and primary sea salt it is
498 inconceivable that a significant amount of primary nitrate can be produced
499 (nitrate is a tracer nutrient in sea water) and, therefore, must be derived by
500 condensation of nitric acid on pre-existing sea salt.

501 Similar relationship was observed for oxalate (top right plot of Figure 5), but
502 there were many more outliers from linear pattern. While oxalate can indeed
503 condense on pre-existing sea salt particles its chemical pathways of secondary
504 production are different and more diverse than that of nitrate as were detailed by
505 Rinaldi et al. (2011). Oxalate can also be present in sea-spray particles via

506 oxidation of organic matter in sea-spray and, therefore, dependent on biological
507 activity of the ocean. As opposed to nitrate, the oxalate was not enhanced in the
508 presence of copious amounts of sea salt particles suggesting that oxalic acid is
509 not an ever present species in the boundary layer which would readily condense
510 on sea salt. The same was true for MSA which showed even less of a relationship
511 with the sea salt mass (bottom left of Figure 5). MSA production is
512 photochemically driven and time limited considering the gradient footprint of
513 0.2-10 km in the coastal zone. The water soluble organic nitrogen (WSON) is a
514 relatively less studied class of chemical compounds of which amines are the best
515 known compounds (Facchini et al., 2008a). The observed concentrations of
516 DEA, DMA and WSON were very similar to the ones documented by Facchini et
517 al. (2008a) in clean marine air masses. Both WSON and the sum of
518 dimethylamine (DMA) and diethylamine (DEA) exhibited a relationship with
519 water soluble organic carbon (WSOC) (bottom right of Figure 5), however, only
520 WSOC and WSON correlated at a significant level ($r = 0.58$). Note, that the sum
521 of amines is presented in absolute concentration while that of WSON as a mass
522 of nitrogen. The comparison between the WSON and the sum of amines
523 suggested that the amines were likely the dominant species of WSON, but
524 difficult to determine due to detection limit as noted above.
525 WSOC/WSON/DEA/DMA relationship is presented in Figure 5 (bottom right)
526 for exploratory purposes as these interrelationships have not been examined or
527 discussed in the context of marine aerosol.

528

529 **3.2 Chemical fluxes**

530

531 **3.2.1 Sea salt flux**

532 The individual concentration profiles had to be fitted first in order to calculate
533 gradients and then fluxes using Equation 1. The concentration gradient is a
534 derivative of the concentration as a function of height. The lowest level at which
535 concentration was measured was at 3 meters and may have been affected by surf-
536 zone fluxes as discussed in detail by Ceburnis et al. (2008). Therefore, only the
537 concentrations measured at 10 and 30m were used in calculating primary fluxes
538 in order to reduce surf-zone related uncertainty in calculated fluxes. This
539 approach yielded “linear gradients” and constant fluxes. It is important to note

540 that for comparison purposes K_z values were adjusted for 10m wind speed from
541 Figure 1 given well established relationship between K_z values and the horizontal
542 wind speed as well as good agreement between EC and gradient samples. Sea
543 salt (SS) and sea-spray (SS+WIOM) flux dependence on the wind speed is
544 presented in Figure 6. The uncertainty parameters of all the fitted flux-wind
545 speed relationships are summarised in Table 3. The obtained relationship was the
546 power law very similar to the one obtained by Ceburnis et al. (2008), but this
547 time it was quantified separately for sea salt and sea-spray. The relationship of
548 sea-spray flux was stronger; however, inherent uncertainty had to be considered.
549 The K_z values were calculated explicitly and, therefore, the uncertainty of the
550 flux was down to the uncertainty of the gradient which in turn was dependent on
551 the accuracy of the chemical analysis. The uncertainty of the individual sea salt
552 fluxes was calculated as a combined propagated uncertainty of the two
553 concentrations (10 and 30m height) and the uncertainty of K_z values. The
554 uncertainty of the fitted relationship was presented as the 95% confidence bands.
555 Typically, the confidence bands would narrow constraining the relationship as
556 the number of points increase and/or their scatter decreases. The power law
557 exponent of SS and sea spray (3.15 & 3.4) source function were very similar to
558 SS source function obtained by Ovadnevaite et al. (2012) who obtained power
559 law exponent of 2.7 using high resolution measurements with aerosol mass
560 spectrometer. The maximum sea salt flux calculated by flux-gradient method was
561 $2\text{-}3 \text{ ng m}^{-2} \text{ s}^{-1}$ at the maximum average wind speed of $11\text{-}12 \text{ m s}^{-1}$ while the mass
562 flux range presented by Ovadnevaite et al. (2012) was $15\text{-}20 \text{ ng m}^{-2} \text{ s}^{-1}$ at 25 m s^{-1}
563 hardly in need of extrapolation to even higher wind speed. However,
564 quantitatively both studies (this study and Ovadnevaite et al. (2012)) agreed well
565 for a given wind speed of e.g. 10 m s^{-1} , 1.67 and $1.97 \text{ ng m}^{-2} \text{ s}^{-1}$, respectively.
566 Only two of the individual fluxes lay outside the 95% confidence bands
567 suggesting that the linear flux-gradient method is not the ideal one - it is an
568 approximation after all. It is suspected that the necessitated long averaging time
569 of the sample was an important reason behind it as well.

570

571 **3.2.1 Organic matter flux**

572 The corresponding chemical flux of WIOM was calculated and presented in
573 Figure 7 (left). All uncertainty considerations are the same for the sea salt and

574 sea-spray fluxes. There was one important difference, however; the WIOM
575 fluxes turned out to be positive only at relatively strong wind speed exceeding 7
576 m s^{-1} while all WIOM fluxes below this value were negative (with consequential
577 large intercept), pointing at the removal or deposition of WIOM. Note, that the
578 negative fluxes corresponding to lower wind speed were obtained from removal
579 profiles introduced previously in chapter 3.1.1. That does not mean that the
580 production flux becomes negative at low wind speed, but rather reflects
581 observations when the production flux at very low wind speed in the gradient
582 footprint area is smaller than the deposition flux of WIOM generated tens to
583 hundreds kilometres away. Therefore, the resulting negative WIOM flux at low
584 wind speed occurred due to the absence of biological activity in the flux footprint
585 area (within ~ 10 km from the measurement location). Another possibility is that
586 there is no measurable concentration increase in WIOM mass at wind speeds
587 below 7 m s^{-1} resulting in the negative flux as WIOM is being removed from the
588 surface layer due to the largely absent source.

589 The WIOM flux was best fitted to the line and there were reasons why it might
590 be so. The WIOM content in sea spray depends on two processes: (1) fractional
591 contribution of OM to sea spray as a function of biological activity and/or
592 organic matter concentration and physico-chemical state in sea water; and (2) sea
593 spray production flux as a function of wind stress or wave state. The two
594 processes are independent and combine differently during different seasons. For
595 example, during summer the fractional contribution of OM is typically higher,
596 but the sea spray flux is typically lower while during winter the production flux
597 would typically be high (due to deeper low pressure systems generating higher
598 wind speeds), but the fractional contribution of OM would be the lowest.

599 The water soluble organic matter exhibited the removal gradient throughout the
600 study period which allowed studying a seasonal pattern of a sink and a
601 dependence on meteorological parameters. Individual WSOM concentration
602 profiles were first fitted to power law using concentrations at all three heights
603 and then the resulting fluxes were calculated by the Equation 1 at 10 meter
604 height. The reason why all three heights were used is that WSOM concentration
605 profiles pointed to a well-established removal profile with the surf-zone having
606 minimal if any impact. The removal rate dependence on the wind speed is
607 presented in Figure 7 (right) and attempted to fit to the power law. It turned out

608 that the WSOM removal rate or sink was dependent on the wind speed with a
609 power law coefficient of 2.2 but with large uncertainty of ~30% (Table 3). Due
610 to the large uncertainty of the individual fluxes the actual removal rate is
611 uncertain too, but the removal rate of WSOM is opposite in sign to WIOM
612 providing hints that a significant fraction of WSOM is in fact processed primary
613 WIOM as has been already proposed (Rinaldi et al., 2010; Decesari et al., 2011).

614

615 **3.3 A comparison with the other flux-wind speed relationships**

616 Given the uncertainty of the derived sea salt flux and wind speed
617 parameterisation it was important to compare it with other available source
618 functions. Equally important was to cover a wide range of methods used to
619 derive fluxes. Figure 8 presents the source functions for which submicron sea salt
620 mass could have been calculated and include the following: Callaghan (2013),
621 Clarke et al. (2006), Fuentes et al. (2010), Gong-Monahan (Gong, 2003),
622 Martensson et al. (2003), Ovadnevaite et al. (2012; 2013) and this study. Clarke
623 et al. (2006), Fuentes et al. (2010) and Martensson et al. (2003) parameterisations
624 were derived in either laboratory conditions or in-situ surf breaking waves and
625 coupled with Monahan and Muircheartaigh (1980) whitecap parameterisation to
626 yield flux wind speed relationship. All of the above parameterisations were based
627 on exploring SMPS measurement data. Gong et al. (2003) used an original
628 Monahan (Monahan et al., 1982) parameterisation obtained in the laboratory
629 experiment and adjusted for the size range $<0.2 \mu\text{m}$. Callaghan (2013) used in-
630 situ whitecap measurements developing a discrete whitecap method and Gong
631 (2003) parameterisation to obtain submicrometer sea salt mass flux and wind
632 speed parameterisation. While the Callaghan (2013) paper proposes a new SSA
633 source function, it pulls the whitecap parameterisation from the Callaghan et al.
634 (2008) paper. One of the primary findings of the Callaghan (2013) work was the
635 importance of choosing the correct whitecap timescale for the discrete whitecap
636 method in particular. Finally, Ovadnevaite et al. (2012; 2013) and flux-gradient
637 method of this study used ambient measurement data (real-time AMS sea salt
638 measurements, SMPS measurements and PM1 gradient measurements,
639 respectively), but were completely independent of each other and different in
640 terms of the utilised methods. It should be noted, that despite the fact that the
641 latter methods estimated net fluxes as opposed to production fluxes measured in

642 the laboratory experiments, deposition fluxes are typically small, in the order of
643 2-4% in submicron particle range (Hoppel et al., 2002). The presented
644 parameterisations fall into two regimes as seen in Figure 9: Clarke et al. (2006),
645 Fuentes et al. (2010), Gong (2003) and Martensson et al. (2003)
646 parameterisations exhibit a significantly higher wind-speed dependency
647 compared to the more recent parameterisations by Callaghan (2013),
648 Ovadnevaite et al. (2012; 2013) and this study. Note, that all the latter
649 parameterisations were based on ambient measurement data. The split into
650 regimes is even more apparent on a linear flux scale. It must be noted that up
651 until now majority of global or regional scale models used one of the former four
652 parameterisations (Gong, 2003; Martensson et al., 2003; Clarke et al., 2006;
653 Fuentes et al., 2010) typically resulting in the overestimated mass concentrations
654 (e.g. (Textor et al., 2006; de Leeuw et al., 2011). Figure 7 reiterates the
655 conclusion made by Ovadnevaite et al. (2012) that the improvements were
656 needed in both whitecap parameterisation, now addressed by Callaghan (2013);
657 and the more realistic differential aerosol productivity term recently advanced by
658 Ovadnevaite et al.(2013). It is reasonable to suggest that the laboratory
659 experiments or the *in-situ* surf breaking waves were most likely unable to
660 realistically replicate air entrainment by the open ocean breaking waves and
661 consequently formed bubble plumes, resulting in unrealistic whitecap coverage
662 and/or size distributions. The most recently developed parameterisation by
663 Ovadnevaite et al. (2013) advanced even further by introducing Reynolds
664 number instead of a commonly used wind speed, thereby removing the
665 uncertainty related to the sea wave state (during rising or waning winds) and
666 implicitly containing sea surface water temperature and salinity which have been
667 both implicated to altering aerosol production (Martensson et al., 2003; Jaegle et
668 al., 2011; Zabori et al., 2012).

669 It can be argued that the new whitecap parameterisation of Callaghan et al.
670 (2013) coupled with Clarke et al. (2006), Fuentes et al. (2010) and Martensson et
671 al. (2003) parameterisations would bring all of them closer to the more recent
672 parameterisations, however, it is important to make few distinctive comments.
673 While the Gong-Monahan parameterisation has decreased the sea salt mass flux
674 when coupled with Callaghan (2013) whitecap parameterisation instead of the
675 original Monahan (Monahan et al., 1982) whitecap parameterisation, the size

676 resolved flux remains unrealistic due to the arbitrary adjusted submicron size
677 distribution below $0.2 \mu\text{m}$ (Gong, 2003). A single mode centred at around 100nm
678 fails to reproducing submicron size distributions observed in ambient air in
679 stormy maritime boundary layer (Ovadnevaite et al., 2013). Similarly, Clarke et
680 al. (2006), Fuentes et al. (2010) and Martensson et al. (2003) parameterisations,
681 even when coupled with Callaghan (2013) whitecap parameterisation, would still
682 predict concentrations far in excess of observed concentrations. The size resolved
683 fluxes are crucial in predicting direct and indirect climate effects and have to be
684 benchmarked against the ambient rather than the laboratory measurements unless
685 both reasonably agree.

686 The most significant limitation of the flux-gradient method is that it allowed
687 calculating fluxes up to moderate wind speed only. It is extremely rare that the
688 average wind speed above 15 m s^{-1} would be sustained over a week period.
689 Therefore, the sea spray source function method proposed by Ovadnevaite et al.
690 (2012; 2013) has to be considered as the more useful source function covering
691 wind speed range of up to 26 m s^{-1} . It should be also noted that the applicability
692 of the Clarke et al.(2006), Fuentes et al. (2010) and Martensson et al. (2003)
693 parameterisations come more questionably for higher wind speeds as the
694 divergence between the more recent parameterisations becomes progressively
695 greater and the slope of the dependency curve becomes unrealistically steep.

696

697 **3.4 WIOM and chlorophyll-a relationship**

698 Gantt et al. (2011) suggested that fractional contribution of organic matter in sea
699 spray particles depends not only on the biological activity in oceanic surface
700 waters, but also the wind speed at the point of emission. The data of this study
701 were examined according to the approach of Gantt et al. (2011). Figure 9
702 presents inter-relationship between fractional organic matter contribution to sea
703 spray ($\text{OM}_{\text{ss}} = \text{WIOM}/(\text{WIOM} + \text{SS})$), wind speed using the data set of this study
704 which were not part of the dataset used by Gantt et al. (2011) and chlorophyll-a
705 concentration in the area upwind from Mace Head as examined in Rinaldi et al.
706 (2013). Only WIOM was taken into account in calculating fractional contribution
707 of OM in sea spray. Notwithstanding the fact that a fraction of measured WSOM
708 was associated with sea spray and formed by processing primary WIOM,
709 quantitative assessment is beyond current knowledge. Both relationships were

710 statistically significant ($P \ll 0.01$) and explained 58% of the variance (top plots)
711 suggesting an overlap. The obtained relationships agree well with the
712 relationship reported by Rinaldi et al. (2013) based on an extended dataset
713 (reaching 70% OM fractional contribution at $1.0 \mu\text{g m}^{-3}$). Further, when the
714 former relationship is coloured by the chlorophyll-a concentration in the oceanic
715 region upfront of the measurement location at Mace Head, no apparent pattern
716 can be discerned (bottom plot) apart from general mutual relationship. It can be
717 concluded, that while the OM_{ss} dependence on wind speed is significant it may
718 actually be weaker than the OM_{ss} and chlorophyll-a relationship due to inter-
719 dependence of wind speed and chlorophyll-a – wind speed is higher in winter
720 when chlorophyll-a concentration is at its lowest and vice versa – thereby
721 contributing to the excessive variance of OM_{ss} and wind speed. Note that
722 seasonal relationship between wind speed and chlorophyll is simply a
723 coincidence. However, it is hardly a coincidence that the two points (top right
724 plot in Figure 9) with rather similar chlorophyll-a concentration ($\sim 0.4 \mu\text{g m}^{-3}$)
725 residing outside the 95% confidence bands are the ones characterised with the
726 lowest and the highest wind speed re-affirming that the effect of wind speed is
727 real, but difficult to separate from the OM_{ss} and chlorophyll-a relationship. Last
728 but not least, it is important to note that the chlorophyll-a concentration is only
729 useful as a proxy of biological activity which can affect a fraction of primary
730 organic matter in sea spray in different ways depending on the trophic level
731 interactions.

732

733 **3.5 Seasonality of observed concentrations, gradients and fluxes**

734 The sampling strategy aimed at capturing two samples per month providing that
735 clean marine conditions were prevailing and each sample lasted on average 50%
736 of time during the calendar week. In reality, fifteen samples were collected
737 covering full year (April 2008 – May 2009) as listed in Table 1. The observed
738 seasonal cycle may not have been typical, but allowed to examine fluxes
739 associated with varying oceanic conditions throughout the calendar year.

740 The observed chemical species concentrations have been typical of those
741 documented at Mace Head by Yoon et al. (2007) and Ovadnevaite et al. (2014).
742 Sea salt concentrations and respective fluxes were generally the largest in winter
743 and the smallest in summer which was mainly due to the wind pattern over the

744 North East Atlantic (Jennings et al., 2003; O'Dowd et al., 2014). However,
745 occurrence of deep low pressure system in e.g. September 2008 with
746 corresponding high winds resulted in high sea salt concentrations and large
747 fluxes despite seasonal pattern suggesting otherwise. Therefore, sea salt fluxes
748 should be considered independent of the season and dependant on the wind
749 speed. On the other hand, it has been suggested that sea salt can be replaced in
750 primary sea spray by primary marine OM (Oppo et al., 1999; Facchini et al.,
751 2008b) in which case sea salt fluxes estimated from observed concentrations
752 would be somewhat diminished. This is at least partially reflected in the
753 differences between sea salt and sea spray fluxes and the larger respective sea
754 spray flux uncertainties. Also, the stronger sea salt and wind speed power law
755 relationship compared to pure sea salt relationship presented in Ovadnevaite et
756 al. (2012) suggests that the smaller sea salt fluxes during summer may be due to
757 the aforementioned replacement effect and may have constrained the relationship
758 to the higher power. Furthermore, Vaishya et al. (2012) showed that aerosol
759 scattering dependence on the wind is different between contrasting seasons
760 suggesting the effect of primary marine OM on sea spray production.

761 The WIOM concentrations and fluxes revealed a much more complex pattern.
762 The absolute concentrations were lower in winter and higher in summer
763 following the pattern of oceanic biological activity lately reaffirmed by
764 Ovadnevaite et al. (2014). The seasonal variation of WIOM gradients and fluxes,
765 however, was different as the gradients depended on biological activity in the
766 flux footprint region (0.2-10 km from the coast) while the fluxes depended both
767 on the biological activity and wind speed dependent sea spray production in the
768 flux footprint area. The three distinct profiles of WIOM gradients presented in
769 Figure 3 clustered in characteristic periods. The removal gradient prevailed in
770 late spring and early summer when biological activity was waning close to the
771 coast. Yoon et al. (2007) demonstrated that biological activity revealed by
772 chlorophyll proxy has been typically starting at the coast early in the season and
773 then gradually moving off-shore and northward, thereby affecting the WIOM
774 gradients and corresponding fluxes. The production gradient manifested itself
775 during late summer and early spring, reaffirming conclusions made by Yoon et
776 al. (2007) about the presence of two or more phytoplankton bloom peaks during
777 the biologically active season. The mixed WIOM profile prevailed during

778 autumn when biological activity was waning over the North East Atlantic, but at
779 the same time shifting closer to the coast. The spatial resolution of satellite
780 chlorophyll data and the large errors associated with coastal interfaces in
781 particular (Darecki and Stramski, 2004; Gregg and Casey, 2007) prevented
782 exploring the relationship between coastal biological activity and WIOM
783 gradients, fluxes and its fractional contribution to sea spray. Previous chapter
784 demonstrated that open ocean biological activity revealed by the chlorophyll
785 proxy upwind from Mace Head correlated well with the WIOM fractional
786 contribution to sea spray validating the seasonal pattern of WIOM gradients and
787 fluxes. Therefore, despite WIOM fluxes were found dependent on biological
788 activity in the flux footprint area (0.2-10km) that did not invalidate a relationship
789 between WIOM and chlorophyll in the open ocean over the North East Atlantic.
790 In summary, the results of this study reaffirmed conclusion made by Ovadnevaite
791 et al. (2013) that their newly developed sea spray source function can be
792 justifiably combined with primary OM parameterisation by chlorophyll proxy of
793 Rinaldi et al. (2013) at least in the North East Atlantic region. Burrows et al.
794 (2014) has recently developed a novel framework trying to reconcile
795 observations from different regions combining fractionation of marine OM with
796 global marine biogeochemistry model. Recently, Long et al. (2014) demonstrated
797 a diurnal signal in primary marine OM production suggesting that sunlight-
798 mediated biogenic surfactants may have a previously overlooked role. However,
799 time resolution of the gradient samples (weekly) and randomness of clean sector
800 sampling during day and night, prevented exploring the effect in this study.
801 However, the results of this study do not contradict the above study either as the
802 primary marine OM production would be enhanced in summer compared to other
803 seasons following radiation pattern.

804

805 **3.6 Boundary layer filling time**

806 The boundary layer filling time helps to understand a conceptual relationship
807 between the species concentration and its corresponding flux. The calculated sea
808 salt fluxes allowed an estimation of an important parameter called boundary
809 layer filling time τ according to the following equation:

$$810 \quad F_{eff} = \frac{C \times H_{MBL}}{\tau} \quad (4)$$

811 where F_{eff} is the effective flux; C is the concentration; H_{MBL} is the height of
812 marine boundary layer.

813

814 The boundary layer filling time for each sampling period was calculated using
815 the measured boundary layer height (day or night providing clean sector
816 condition were met), calculated sea salt flux (Figure 6) and the absolute sea salt
817 concentration at 30m level assumed as representative of the well mixed boundary
818 layer. The surface mixed layer (SML) height obtained from LIDAR
819 measurements varied in the range of 846-1102 meters among the eight periods
820 for which overlapping LIDAR measurements were available. An occasional
821 formation of nocturnal boundary layer was ignored here due to the nature and
822 resolution of the gradient samples. The corresponding filling time range was
823 calculated as 0.9-5.1 days with the median value of 1.8 days. Similar values of
824 the time constant to reach equilibrium concentration in the boundary layer taking
825 into consideration particle sizes were obtained by Hoppel et al. (2002) and the
826 value of 2 used by Ovadnevaite et al. (2012) in calculating the sea salt mass flux
827 based on sea salt concentration measurement. It is important to note, however,
828 that the filling time constant is a feature of a particular low pressure system
829 arriving at the point of observation in a connecting flow. Moreover, the flux-
830 gradient method is independent of the filling time and pretty insensitive to
831 precipitation which would mainly affect the absolute concentration value not
832 used in this study (concentration gradient was used instead). All other things
833 equal, the absolute concentration in the well mixed boundary layer would
834 continuously increase at a given flux eventually reaching steady state. Figure 10
835 helps to visualise various relationships between the four parameters: sea salt
836 concentration, sea salt flux, wind speed and boundary layer filling time. The
837 shortest filling time was obtained for the periods of the highest flux when the
838 absolute concentration was at its lowest. Clearly, the strongest winds could not
839 be sustained over the long periods of time to achieve a proportionally high
840 absolute mass concentration.

841 The longest boundary layer filling times should be attributed to the series of
842 well-defined low pressure systems without significant precipitation and the
843 calculated flux should be representative of the entire region of concentration

844 footprint which is many tens to few hundred kilometres upwind from Mace Head
845 (Ceburnis et al., 2008).

846

847 **4 Conclusions**

848 Marine aerosol sources, sinks and chemical fluxes were studied over the entire
849 year by the gradient method. The chemical fluxes of primary species, such as sea
850 salt, and more generally sea-spray were found to show strong power law
851 relationship with the wind speed. The power law exponent of sea salt mass
852 source function was 3.15 which was fractionally higher than the generally
853 considered cubic power law relationship. The flux versus wind speed relationship
854 of WIOM was found to be linear resulting from a dependence on the biological
855 activity in oceanic waters as supported by the linear dependence of fractional
856 contribution of organic matter on chlorophyll-a concentration and the power law
857 relationship of sea spray production. The study of certain secondary species
858 (nitrate, oxalate, MSA, WSON) was performed for the first time revealing their
859 mainly secondary origin, but also interactions with primary sea spray. The
860 seasonal pattern of concentrations, gradients and corresponding fluxes
861 highlighted complex interactions between biological activity, especially in the
862 flux footprint area, and wind driven sea spray production. The marine boundary
863 layer filling time was found to be variable in the range of 1 to 5 days linking
864 species concentration, flux and wind speed. The obtained sea salt mass flux and
865 wind speed parameterisation compared very well with other parameterisations
866 which used carefully selected ambient measurement data. The comparison with
867 the range of available flux-wind-speed parameterisations revealed significant
868 advances in the development of the sea spray source function for the benefit of
869 global climate models.

870

871 **Acknowledgements**

872 The work of this paper has been funded by the EPA Ireland STRIVE project
873 EASI-AQCIS and D. Ceburnis fellowship project Research Support for Mace
874 Head. The European Space Agency (Support To Science Element: Oceanflux
875 Sea Spray Aerosol) and EC ACTRIS Research Infrastructure Action under the
876 7th Framework Programme support are acknowledged as well. The authors
877 would like to thank A. Callaghan from Scripps Institution of Oceanography,

878 USA for sharing his data; Salvatore Marullo from Italian National Agency for
879 New Technologies, Energy and Sustainable Economic Development (ENEA),
880 Frascati, Italy and Rosalia Santoleri from Institute of Atmospheric Sciences and
881 Climate, National Research Council, Rome, Italy for providing satellite
882 chlorophyll data.
883

884 **References**

- 885 Ahlm, L., Nilsson, E. D., Krejci, R., Martensson, E. M., Vogt, M., and Artaxo,
886 P.: Aerosol number fluxes over the Amazon rain forest during the wet season,
887 *Atmos. Chem. Phys.*, 9, 9381-9400, 2009.
- 888 Blanchard, D. C.: Sea-to-air transport of surface active material, *Science*, 146,
889 396-397, 1964.
- 890 Brooks, I. M., Yelland, M. J., Upstill-Goddard, R. C., Nightingale, P. D., Archer,
891 S., d'Asaro, E., Beale, R., Beatty, C., Blomquist, B., Bloom, A. A., Brooks, B. J.,
892 Cluderay, J., Coles, D., Dacey, J., DeGrandpre, M., Dixon, J., Drennan, W. M.,
893 Gabriele, J., Goldson, L., Hardman-Mountford, N., Hill, M. K., Horn, M., Hsueh,
894 P. C., Huebert, B., de Leeuw, G., Leighton, T. G., Liddicoat, M., Lingard, J. J.
895 N., McNeil, C., McQuaid, J. B., Moat, B. I., Moore, G., Neill, C., Norris, S. J.,
896 O'Doherty, S., Pascal, R. W., Prytherch, J., Rebozo, M., Sahlee, E., Salter, M.,
897 Schuster, U., Skjelvan, I., Slagter, H., Smith, M. H., Smith, P. D., Srokosz, M.,
898 Stephens, J. A., Taylor, P. K., Telszewski, M., Walsh, R., Ward, B., Woolf, D.
899 K., Young, D., and Zemmelenk, H.: Physical Exchanges at the Air-Sea Interface
900 Uk-Solas Field Measurements, *Bulletin of the American Meteorological Society*,
901 90, 629-644, 10.1175/2008bams2578.1, 2009.
- 902 Burrows, S. M., Ogunro, O., Frossard, A. A., Russell, L. M., Rasch, P. J., and
903 Elliott, S. M.: A physically based framework for modeling the organic
904 fractionation of sea spray aerosol from bubble film Langmuir equilibria, *Atmos.*
905 *Chem. Phys.*, 14, 13601-13629, 10.5194/acp-14-13601-2014, 2014.
- 906 Buzorius, G., Rannik, U., Makela, J. M., Vesala, T., and Kulmala, M.: Vertical
907 aerosol particle fluxes measured by eddy covariance technique using
908 condensational particle counter, *Journal of Aerosol Science*, 29, 157-171,
909 10.1016/s0021-8502(97)00458-8, 1998.
- 910 Callaghan, A., de Leeuw, G., Cohen, L., and O'Dowd, C. D.: Relationship of
911 oceanic whitecap coverage to wind speed and wind history, *Geophys. Res. Lett.*,
912 35, L23609,
913 10.1029/2008gl036165, 2008.
- 914 Callaghan, A. H.: An improved whitecap timescale for sea spray aerosol
915 production flux modeling using the discrete whitecap method, *J. Geophys. Res.-*
916 *Atmos.*, 118, 9997-10010, 10.1002/jgrd.50768, 2013.
- 917 Cavalli, F., Facchini, M. C., Decesari, S., Mircea, M., Emblico, L., Fuzzi, S.,
918 Ceburnis, D., Yoon, Y. J., O'Dowd, C. D., Putaud, J. P., and Dell'Acqua, A.:
919 Advances in characterization of size-resolved organic matter in marine aerosol
920 over the North Atlantic, *J. Geophys. Res.-Atmos.*, 109, D24215,
921 10.1029/2004jd005137, 2004.
- 922 Ceburnis, D., Garbaras, A., Szidat, S., Rinaldi, M., Fahrni, S., Perron, N.,
923 Wacker, L., Leinert, S., Remeikis, V., Facchini, M. C., Prevot, A. S. H.,
924 Jennings, S. G., Ramonet, M., and O'Dowd, C. D.: Quantification of the
925 carbonaceous matter origin in submicron marine aerosol by C-13 and C-14

- 926 isotope analysis, *Atmos. Chem. Phys.*, 11, 8593-8606, 10.5194/acp-11-8593-
927 2011, 2011.
- 928 Ceburnis, D., O'Dowd, C. D., Jennings, G. S., Facchini, M. C., Emblico, L.,
929 Decesari, S., Fuzzi, S., and Sakalys, J.: Marine aerosol chemistry gradients:
930 Elucidating primary and secondary processes and fluxes, *Geophys. Res. Lett.*, 35,
931 L07804, 10.1029/2008gl033462, 2008.
- 932 Charlson, R. J., Lovelock, J. E., Andreae, M. O., and Warren, S. G.: Oceanic
933 phytoplankton, atmospheric sulfur, cloud albedo and climate, *Nature*, 326, 655-
934 661, 1987.
- 935 Clarke, A. D., Owens, S. R., and Zhou, J. C.: An ultrafine sea-salt flux from
936 breaking waves: Implications for cloud condensation nuclei in the remote marine
937 atmosphere, *J. Geophys. Res.-Atmos.*, 111, 10.1029/2005jd006565, 2006.
- 938 Coe, H., Allan, J. D., Alfarra, M. R., Bower, K. N., Flynn, M. J., McFiggans, G.
939 B., Topping, D. O., Williams, P. I., O'Dowd, C. D., Dall'Osto, M., Beddows, D.
940 C. S., and Harrison, R. M.: Chemical and physical characteristics of aerosol
941 particles at a remote coastal location, Mace Head, Ireland, during NAMBLEX,
942 *Atmos. Chem. Phys.*, 6, 3289-3301, 2006.
- 943 Cooke, W. F., Jennings, S. G., and Spain, T. G.: Black carbon measurements at
944 Mace Head, 1989-1996, *J. Geophys. Res.-Atmos.*, 102, 25339-25346,
945 10.1029/97jd01430, 1997.
- 946 Dall'Osto, M., Ceburnis, D., Monahan, C., Worsnop, D. R., Bialek, J., Kulmala,
947 M., Kurten, T., Ehn, M., Wenger, J., Sodeau, J., Healy, R., and O'Dowd, C.:
948 Nitrogenated and aliphatic organic vapors as possible drivers for marine
949 secondary organic aerosol growth, *J. Geophys. Res.-Atmos.*, 117,
950 10.1029/2012jd017522, 2012.
- 951 Darecki, M., and Stramski, D.: An evaluation of MODIS and SeaWiFS bio-
952 optical algorithms in the Baltic Sea, *Remote Sensing of Environment*, 89, 326-
953 350, 10.1016/j.rse.2003.10.012, 2004.
- 954 de Leeuw, G., Andreas, E. L., Anguelova, M. D., Fairall, C. W., Lewis, E. R.,
955 O'Dowd, C., Schulz, M., and Schwartz, S. E.: Production flux of sea spray
956 aerosol, *Reviews of Geophysics*, 49, Rg2001, 10.1029/2010rg000349, 2011.
- 957 Decesari, S., Finessi, E., Rinaldi, M., Paglione, M., Fuzzi, S., Stephanou, E. G.,
958 Tziaras, T., Spyros, A., Ceburnis, D., O'Dowd, C., Dall'Osto, M., Harrison, R.
959 M., Allan, J., Coe, H., and Facchini, M. C.: Primary and secondary marine
960 organic aerosols over the North Atlantic Ocean during the MAP experiment, *J.*
961 *Geophys. Res.-Atmos.*, 116, D22210, 10.1029/2011jd016204, 2011.
- 962 Decesari, S., Mircea, M., Cavalli, F., Fuzzi, S., Moretti, F., Tagliavini, E., and
963 Facchini, M. C.: Source attribution of water-soluble organic aerosol by nuclear
964 magnetic resonance spectroscopy, *Environ. Sci. Technol.*, 41, 2479-2484, Doi
965 10.1021/Es061711l, 2007.

- 966 Facchini, M. C., Decesari, S., Rinaldi, M., Carbone, C., Finessi, E., Mircea, M.,
967 Fuzzi, S., Moretti, F., Tagliavini, E., Ceburnis, D., and O'Dowd, C. D.: Important
968 Source of Marine Secondary Organic Aerosol from Biogenic Amines, *Environ.*
969 *Sci. Technol.*, 42, 9116-9121, 10.1021/Es8018385, 2008a.
- 970 Facchini, M. C., Rinaldi, M., Decesari, S., Carbone, C., Finessi, E., Mircea, M.,
971 Fuzzi, S., Ceburnis, D., Flanagan, R., Nilsson, E. D., de Leeuw, G., Martino, M.,
972 Woeltjen, J., and O'Dowd, C. D.: Primary submicron marine aerosol dominated
973 by insoluble organic colloids and aggregates, *Geophys. Res. Lett.*, 35, L17814,
974 10.1029/2008gl034210, 2008b.
- 975 Farmer, D. K., Kimmel, J. R., Phillips, G., Docherty, K. S., Worsnop, D. R.,
976 Sueper, D., Nemitz, E., and Jimenez, J. L.: Eddy covariance measurements with
977 high-resolution time-of-flight aerosol mass spectrometry: a new approach to
978 chemically resolved aerosol fluxes, *Atmospheric Measurement Techniques*, 4,
979 1275-1289, 10.5194/amt-4-1275-2011, 2011.
- 980 Fratini, G., Ciccioli, P., Febo, A., Forgione, A., and Valentini, R.: Size-
981 segregated fluxes of mineral dust from a desert area of northern China by eddy
982 covariance, *Atmos. Chem. Phys.*, 7, 2839-2854, 2007.
- 983 Fuentes, E., Coe, H., Green, D., de Leeuw, G., and McFiggans, G.: On the
984 impacts of phytoplankton-derived organic matter on the properties of the primary
985 marine aerosol - Part 1: Source fluxes, *Atmos. Chem. Phys.*, 10, 9295-9317, DOI
986 10.5194/acp-10-9295-2010, 2010.
- 987 Gaman, A., Rannik, U., Aalto, P., Pohja, T., Siivola, E., Kulmala, M., and
988 Vesala, T.: Relaxed eddy accumulation system for size-resolved aerosol particle
989 flux measurements, *Journal of Atmospheric and Oceanic Technology*, 21, 933-
990 943, 10.1175/1520-0426, 2004.
- 991 Gantt, B., Meskhidze, N., Facchini, M. C., Rinaldi, M., Ceburnis, D., and
992 O'Dowd, C.: Wind speed dependent size-resolved parameterization for the
993 organic mass fraction of sea spray aerosol, *Atmos. Chem. Phys.*, 11, 8777-8790,
994 10.5194/acp-11-8777-2011, 2011.
- 995 Geever, M., O'Dowd, C. D., van Ekeren, S., Flanagan, R., Nilsson, E. D., de
996 Leeuw, G., and Rannik, U.: Submicron sea spray fluxes, *Geophys. Res. Lett.*, 32,
997 Artn L15810, 10.1029/2005gl023081, 2005.
- 998 Gong, S. L.: A parameterization of sea-salt aerosol source function for sub- and
999 super-micron particles, *Glob. Biogeochem. Cycle*, 17, 10.1029/2003gb002079,
1000 2003.
- 1001 Gregg, W. W., and Casey, N. W.: Sampling biases in MODIS and SeaWiFS
1002 ocean chlorophyll data, *Remote Sensing of Environment*, 111, 25-35,
1003 10.1016/j.rse.2007.03.008, 2007.
- 1004 Haeffelin, M., Angelini, F., Morille, Y., Martucci, G., Frey, S., Gobbi, G. P.,
1005 Lolli, S., O'Dowd, C. D., Sauvage, L., Xueref-Remy, I., Wastine, B., and Feist,
1006 D. G.: Evaluation of Mixing-Height Retrievals from Automatic Profiling Lidars

- 1007 and Ceilometers in View of Future Integrated Networks in Europe, *Bound.-Layer*
1008 *Meteor.*, 143, 49-75, 10.1007/s10546-011-9643-z, 2012.
- 1009 Heard, D. E., Read, K. A., Methven, J., Al-Haider, S., Bloss, W. J., Johnson, G.
1010 P., Pilling, M. J., Seakins, P. W., Smith, S. C., Sommariva, R., Stanton, J. C.,
1011 Still, T. J., Ingham, T., Brooks, B., De Leeuw, G., Jackson, A. V., McQuaid, J.
1012 B., Morgan, R., Smith, M. H., Carpenter, L. J., Carslaw, N., Hamilton, J.,
1013 Hopkins, J. R., Lee, J. D., Lewis, A. C., Purvis, R. M., Wevill, D. J., Brough, N.,
1014 Green, T., Mills, G., Penkett, S. A., Plane, J. M. C., Saiz-Lopez, A., Worton, D.,
1015 Monks, P. S., Fleming, Z., Rickard, A. R., Alfarra, M. R., Allan, J. D., Bower,
1016 K., Coe, H., Cubison, M., Flynn, M., McFiggans, G., Gallagher, M., Norton, E.
1017 G., O'Dowd, C. D., Shillito, J., Topping, D., Vaughan, G., Williams, P., Bitter,
1018 M., Ball, S. M., Jones, R. L., Povey, I. M., O'Doherty, S., Simmonds, P. G.,
1019 Allen, A., Kinnersley, R. P., Beddows, D. C. S., Dall'Osto, M., Harrison, R. M.,
1020 Donovan, R. J., Heal, M. R., Jennings, S. G., Noone, C., and Spain, G.: The
1021 North Atlantic Marine Boundary Layer Experiment (NAMBLEX). Overview of
1022 the campaign held at Mace Head, Ireland, in summer 2002, *Atmos. Chem. Phys.*,
1023 6, 2241-2272, 2006.
- 1024 Held, A., Niessner, R., Bosveld, F., Wrzesinsky, T., and Klemm, O.: Evaluation
1025 and application of an electrical low pressure impactor in disjunct eddy
1026 covariance aerosol flux measurements, *Aerosol Science and Technology*, 41,
1027 510-519, 10.1080/02786820701227719, 2007.
- 1028 Hoffman, E. J., and Duce, R. A.: Organic-carbon in marine atmospheric
1029 particulate matter - concentration and particle-size distribution, *Geophys. Res.*
1030 *Lett.*, 4, 449-452, 1977.
- 1031 Hopkins, R. J., Desyaterik, Y., Tivanski, A. V., Zaveri, R. A., Berkowitz, C. M.,
1032 Tyliczszak, T., Gilles, M. K., and Laskin, A.: Chemical speciation of sulfur in
1033 marine cloud droplets and particles: Analysis of individual particles from the
1034 marine boundary layer over the California current, *J. Geophys. Res.-Atmos.*, 113,
1035 10.1029/2007jd008954, 2008.
- 1036 Hoppel, W. A., Frick, G. M., and Fitzgerald, J. W.: Surface source function for
1037 sea-salt aerosol and aerosol dry deposition to the ocean surface, *J. Geophys.*
1038 *Res.-Atmos.*, 107, 4382, 10.1029/2001jd002014, 2002.
- 1039 Jaegle, L., Quinn, P. K., Bates, T. S., Alexander, B., and Lin, J. T.: Global
1040 distribution of sea salt aerosols: new constraints from in situ and remote sensing
1041 observations, *Atmos. Chem. Phys.*, 11, 3137-3157, 10.5194/acp-11-3137-2011,
1042 2011.
- 1043 Jennings, S. G., Kleefeld, C., O'Dowd, C. D., Junker, C., Spain, T. G., O'Brien,
1044 P., Roddy, A. F., and O'Connor, T. C.: Mace head atmospheric research station
1045 characterization of aerosol radiative parameters, *Boreal Environment Research*,
1046 8, 303-314, 2003.
- 1047 Kawamura, K., and Sakaguchi, F.: Molecular distributions of water soluble
1048 dicarboxylic acids in marine aerosols over the Pacific Ocean including tropics, *J.*
1049 *Geophys. Res.-Atmos.*, 104, 3501-3509, 1999.

- 1050 Keane-Brennan, J.: Air to sea gas exchange of CO₂ in the north-east Atlantic
1051 Ocean, PhD Thesis, 2011.
- 1052 Keene, W. C., Maring, H., Maben, J. R., Kieber, D. J., Pszenny, A. A. P., Dahl,
1053 E. E., Izaguirre, M. A., Davis, A. J., Long, M. S., Zhou, X. L., Smoydzin, L., and
1054 Sander, R.: Chemical and physical characteristics of nascent aerosols produced
1055 by bursting bubbles at a model air-sea interface, *J. Geophys. Res.-Atmos.*, 112,
1056 D21202
1057 10.1029/2007jd008464, 2007.
- 1058 Leck, C., and Bigg, E. K.: Source and evolution of the marine aerosol - A new
1059 perspective, *Geophys. Res. Lett.*, 32, L19803, 10.1029/2005gl023651, 2005.
- 1060 Long, M. S., Keene, W. C., Kieber, D. J., Frossard, A. A., Russell, L. M.,
1061 Maben, J. R., Kinsey, J. D., Quinn, P. K., and Bates, T. S.: Light-enhanced
1062 primary marine aerosol production from biologically productive seawater,
1063 *Geophys. Res. Lett.*, 41, 2014GL059436, 10.1002/2014GL059436, 2014.
- 1064 Martensson, E. M., Nilsson, E. D., Buzorius, G., and Johansson, C.: Eddy
1065 covariance measurements and parameterisation of traffic related particle
1066 emissions in an urban environment, *Atmos. Chem. Phys.*, 6, 769-785, 2006.
- 1067 Martensson, E. M., Nilsson, E. D., de Leeuw, G., Cohen, L. H., and Hansson, H.
1068 C.: Laboratory simulations and parameterization of the primary marine aerosol
1069 production, *J. Geophys. Res.-Atmos.*, 108, 4297,
1070 10.1029/2002jd002263, 2003.
- 1071 Martin, C. L., Longley, I. D., Dorsey, J. R., Thomas, R. M., Gallagher, M. W.,
1072 and Nemitz, E.: Ultrafine particle fluxes above four major European cities,
1073 *Atmos. Environ.*, 43, 4714-4721, 10.1016/j.atmosenv.2008.10.009, 2009.
- 1074 Meng, Z., and Seinfeld, J. H.: Time scales to achieve atmospheric gas-aerosol
1075 equilibrium for volatile species, *Atmos. Environ.*, 30, 2889-2900,
1076 [http://dx.doi.org/10.1016/1352-2310\(95\)00493-9](http://dx.doi.org/10.1016/1352-2310(95)00493-9), 1996.
- 1077 Middlebrook, A. M., Murphy, D. M., and Thomson, D. S.: Observations of
1078 organic material in individual marine particles at Cape Grim during the First
1079 Aerosol Characterization Experiment (ACE 1), *J. Geophys. Res.-Atmos.*, 103,
1080 16475-16483, 1998.
- 1081 Milroy, C., Martucci, G., Lolli, S., Loaec, S., Sauvage, L., Xueref-Remy, I.,
1082 Lavric, J. V., Ciais, P., Feist, D. G., Biavati, G., and O'Dowd, C. D.: An
1083 Assessment of Pseudo-Operational Ground-Based Light Detection and Ranging
1084 Sensors to Determine the Boundary-Layer Structure in the Coastal Atmosphere,
1085 *Adv. Meteorol.*, 10.1155/2012/929080, 2012.
- 1086 Mochida, M., Kitamori, Y., Kawamura, K., Nojiri, Y., and Suzuki, K.: Fatty
1087 acids in the marine atmosphere: Factors governing their concentrations and
1088 evaluation of organic films on sea-salt particles, *J. Geophys. Res.-Atmos.*, 107,
1089 4325, 10.1029/2001jd001278, 2002.

- 1090 Monahan, E. C., Davidson, K. L., and Spiel, D. E.: Whitecap Aerosol
1091 Productivity Deduced from Simulation Tank Measurements, *Journal of*
1092 *Geophysical Research-Oceans and Atmospheres*, 87, 8898-8904, 1982.
- 1093 Monahan, E. C., and Muircheartaigh, I. O.: Optimal Power-Law Description of
1094 Oceanic Whitecap Coverage Dependence on Wind-Speed, *J Phys Oceanogr*, 10,
1095 2094-2099, 1980.
- 1096 Muller, C., Iinuma, Y., Karstensen, J., van Pinxteren, D., Lehmann, S., Gnauk,
1097 T., and Herrmann, H.: Seasonal variation of aliphatic amines in marine sub-
1098 micrometer particles at the Cape Verde islands, *Atmos. Chem. Phys.*, 9, 9587-
1099 9597, 2009.
- 1100 Nemitz, E., Jimenez, J. L., Huffman, J. A., Ulbrich, I. M., Canagaratna, M. R.,
1101 Worsnop, D. R., and Guenther, A. B.: An eddy-covariance system for the
1102 measurement of surface/atmosphere exchange fluxes of submicron aerosol
1103 chemical species - First application above an urban area, *Aerosol Science and*
1104 *Technology*, 42, 636-657, 10.1080/02786820802227352, 2008.
- 1105 Nilsson, E. D., Rannik, U., Kulmala, M., Buzorius, G., and O'Dowd, C. D.:
1106 Effects of continental boundary layer evolution, convection, turbulence and
1107 entrainment, on aerosol formation, *Tellus Ser. B-Chem. Phys. Meteorol.*, 53,
1108 441-461, 2001.
- 1109 Norris, S. J., Brooks, I. M., de Leeuw, G., Smith, M. H., Moerman, M., and
1110 Lingard, J. J. N.: Eddy covariance measurements of sea spray particles over the
1111 Atlantic Ocean, *Atmos. Chem. Phys.*, 8, 555-563, 2008.
- 1112 Norton, E. G., Vaughan, G., Methven, J., Coe, H., Brooks, B., Gallagher, M., and
1113 Longley, I.: Boundary layer structure and decoupling from synoptic scale flow
1114 during NAMBLEX, *Atmos. Chem. Phys.*, 6, 433-445, 2006.
- 1115 O'Connor, T. C., Jennings, S. G., and O'Dowd, C. D.: Highlights of fifty years of
1116 atmospheric aerosol research at Mace Head, *Atmospheric Research*, 90, 338-355,
1117 10.1016/j.atmosres.2008.08.014, 2008.
- 1118 O'Dowd, C., Ceburnis, D., Ovadnevaite, J., Vaishya, A., Rinaldi, M., and
1119 Facchini, M. C.: Do anthropogenic, continental or coastal aerosol sources impact
1120 on a marine aerosol signature at Mace Head?, *Atmos. Chem. Phys.*, 14, 10687-
1121 10704, 10.5194/acp-14-10687-2014, 2014.
- 1122 O'Dowd, C. D., and De Leeuw, G.: Marine aerosol production: a review of the
1123 current knowledge, *Philosophical Transactions of the Royal Society a-*
1124 *Mathematical Physical and Engineering Sciences*, 365, 1753-1774,
1125 10.1098/rsta.2007.2043, 2007.
- 1126 O'Dowd, C. D., Facchini, M. C., Cavalli, F., Ceburnis, D., Mircea, M., Decesari,
1127 S., Fuzzi, S., Yoon, Y. J., and Putaud, J. P.: Biogenically driven organic
1128 contribution to marine aerosol, *Nature*, 431, 676-680, 10.1038/Nature02959,
1129 2004.

- 1130 O'Dowd, C. D., Langmann, B., Varghese, S., Scannell, C., Ceburnis, D., and
1131 Facchini, M. C.: A combined organic-inorganic sea-spray source function,
1132 *Geophys. Res. Lett.*, 35, L01801, 10.1029/2007gl030331, 2008.
- 1133 O'Dowd, C. D., Lowe, J. A., and Smith, M. H.: The effect of clouds on aerosol
1134 growth in the rural atmosphere, *Atmospheric Research*, 54, 201-221, 2000.
- 1135 O'Dowd, C. D., Smith, M. H., Consterdine, I. E., and Lowe, J. A.: Marine
1136 aerosol, sea-salt, and the marine sulphur cycle: A short review, *Atmos. Environ.*,
1137 31, 73-80, 1997.
- 1138 Oppo, C., Bellandi, S., Innocenti, N. D., Stortini, A. M., Loglio, G., Schiavuta,
1139 E., and Cini, R.: Surfactant components of marine organic matter as agents for
1140 biogeochemical fractionation and pollutant transport via marine aerosols, *Marine
1141 Chemistry*, 63, 235-253, 1999.
- 1142 Ovadnevaite, J., Ceburnis, D., Canagaratna, M., Berresheim, H., Bialek, J.,
1143 Martucci, G., Worsnop, D. R., and O'Dowd, C.: On the effect of wind speed on
1144 submicron sea salt mass concentrations and source fluxes, *J. Geophys. Res.-
1145 Atmos.*, 117, 10.1029/2011jd017379, 2012.
- 1146 Ovadnevaite, J., Ceburnis, D., Leinert, S., Dall'Osto, M., Canagaratna, M.,
1147 O'Doherty, S., Berresheim, H., and O'Dowd, C.: Submicron NE Atlantic marine
1148 aerosol chemical composition and abundance: Seasonal trends and air mass
1149 categorization, *J. Geophys. Res.-Atmos.*, 119, 11850-11863,
1150 10.1002/2013jd021330, 2014.
- 1151 Ovadnevaite, J., Manders, A., de Leeuw, G., Monahan, C., Ceburnis, D., and
1152 O'Dowd, C. D.: A sea spray aerosol flux parameterization encapsulating wave
1153 state, *Atmos. Chem. Phys. Discuss.*, 13, 23139-23171, 10.5194/acpd-13-23139-
1154 2013, 2013.
- 1155 Rinaldi, M., Decesari, S., Carbone, C., Finessi, E., Fuzzi, S., Ceburnis, D.,
1156 O'Dowd, C. D., Sciare, J., Burrows, J. P., Vrekoussis, M., Ervens, B., Tsigaridis,
1157 K., and Facchini, M. C.: Evidence of a natural marine source of oxalic acid and a
1158 possible link to glyoxal, *J. Geophys. Res.-Atmos.*, 116, D16204,
1159 10.1029/2011jd015659, 2011.
- 1160 Rinaldi, M., Decesari, S., Finessi, E., Giulianelli, L., Carbone, C., Fuzzi, S.,
1161 O'Dowd, C. D., Ceburnis, D., and Facchini, M. C.: Primary and secondary
1162 organic marine aerosol and oceanic biological activity: recent results and new
1163 perspectives for future studies, *Adv. Meteorol.*, 2010, Article ID 310682, 310610
1164 pages, 2010.
- 1165 Rinaldi, M., Facchini, M. C., Decesari, S., Carbone, C., Finessi, E., Mircea, M.,
1166 Fuzzi, S., Ceburnis, D., Ehn, M., Kulmala, M., de Leeuw, G., and O'Dowd, C.
1167 D.: On the representativeness of coastal aerosol studies to open ocean studies:
1168 Mace Head - a case study, *Atmos. Chem. Phys.*, 9, 9635-9646, 2009.
- 1169 Rinaldi, M., Fuzzi, S., Decesari, S., Marullo, S., Santoleri, R., Provenzale, A.,
1170 von Hardenberg, J., Ceburnis, D., Vaishya, A., O'Dowd, C. D., and Facchini, M.

- 1171 C.: Is chlorophyll-a the best surrogate for organic matter enrichment in
1172 submicron primary marine aerosol?, *J. Geophys. Res.-Atmos.*, 118, 4964-4973,
1173 10.1002/jgrd.50417, 2013.
- 1174 Russell, L. M., Hawkins, L. N., Frossard, A. A., Quinn, P. K., and Bates, T. S.:
1175 Carbohydrate-like composition of submicron atmospheric particles and their
1176 production from ocean bubble bursting, *Proceedings of the National Academy of
1177 Sciences of the United States of America*, 107, 6652-6657,
1178 10.1073/pnas.0908905107, 2010.
- 1179 Sciare, J., Favez, O., Sarda-Esteve, R., Oikonomou, K., Cachier, H., and Kazan,
1180 V.: Long-term observations of carbonaceous aerosols in the Austral Ocean
1181 atmosphere: Evidence of a biogenic marine organic source, *J. Geophys. Res.-
1182 Atmos.*, 114, D15302, 10.1029/2009jd011998, 2009.
- 1183 Seinfeld, J. H., and Pandis, S. N.: *Atmospheric chemistry and physics – from air
1184 pollution to climate change* Wiley Interscience, New York, 1232 pp., 2006.
- 1185 Stull, R. B.: *An Introduction to Boundary Layer Meteorology*, Springer, Boston,
1186 680 pp., 1988.
- 1187 Textor, C., Schulz, M., Guibert, S., Kinne, S., Balkanski, Y., Bauer, S., Berntsen,
1188 T., Berglen, T., Boucher, O., Chin, M., Dentener, F., Diehl, T., Easter, R.,
1189 Feichter, H., Fillmore, D., Ghan, S., Ginoux, P., Gong, S., Kristjansson, J. E.,
1190 Krol, M., Lauer, A., Lamarque, J. F., Liu, X., Montanaro, V., Myhre, G., Penner,
1191 J., Pitari, G., Reddy, S., Seland, O., Stier, P., Takemura, T., and Tie, X.: Analysis
1192 and quantification of the diversities of aerosol life cycles within AeroCom,
1193 *Atmos. Chem. Phys.*, 6, 1777-1813, 2006.
- 1194 Turekian, V. C., Macko, S. A., and Keene, W. C.: Concentrations, isotopic
1195 compositions, and sources of size-resolved, particulate organic carbon and
1196 oxalate in near-surface marine air at Bermuda during spring, *J. Geophys. Res.-
1197 Atmos.*, 108, 4157, 10.1029/2002jd002053, 2003.
- 1198 Vaishya, A., Jennings, S. G., and O'Dowd, C.: Wind-driven influences on aerosol
1199 light scattering in north-east Atlantic air, *Geophys. Res. Lett.*, 39,
1200 10.1029/2011gl050556, 2012.
- 1201 Valiulis, D., Ceburnis, D., Sakalys, J., and Kvietkus, K.: Estimation of
1202 atmospheric trace metal emissions in Vilnius City, Lithuania, using vertical
1203 concentration gradient and road tunnel measurement data, *Atmos. Environ.*, 36,
1204 6001-6014, Pii S1352-2310(02)00764-1, 2002.
- 1205 Yoon, Y. J., Ceburnis, D., Cavalli, F., Jourdan, O., Putaud, J. P., Facchini, M. C.,
1206 Decesari, S., Fuzzi, S., Sellegri, K., Jennings, S. G., and O'Dowd, C. D.:
1207 Seasonal characteristics of the physicochemical properties of North Atlantic
1208 marine atmospheric aerosols, *J. Geophys. Res.-Atmos.*, 112, D04206,
1209 10.1029/2005jd007044, 2007.
- 1210 Zabori, J., Matisans, M., Krejci, R., Nilsson, E. D., and Strom, J.: Artificial
1211 primary marine aerosol production: a laboratory study with varying water

1212 temperature, salinity, and succinic acid concentration, Atmos. Chem. Phys., 12,
1213 10709-10724, 10.5194/acp-12-10709-2012, 2012.
1214
1215

1216 Table 1. Gradient sample weekly collection time scale and number of hours each
 1217 sample was sampled during 13 month period in 2008-2009.

10-15/04/2008	36.8	30/06-07/07/2008	24.4	11-18/12/2008	72.8
24-29/04/2008	72.6	14-22/07/2008	147.5	14-21/01/2009	74.8
29/04-07/05/2008	10.3	22-29/08/2008	146.5	25/02-04/03/2009	131.5
27/05-06/06/2008	53.0	08-18/09/2008	84.0	04-11/03/2009	121.5
25/06-30/06/2008	69.3	30/09-10/10/2008	106.7	05-12/05/2009	87.7

1218

1219

1220 Table 2. Absolute concentration ranges of measured chemical species.

Chemical species	Concentration range, $\mu\text{g m}^{-3}$
Sea salt (SS)	0.066-2.571
Nss SO ₄	0.042-0.829
NO ₃	0.001-0.037
NH ₄	0.001-0.127
MSA	0.002-0.428
WSOM	0.047-1.568
WIOM	0.061-0.990
WSON	0.001-0.071
DMA	0.001-0.052
DEA	0.001-0.082
Oxalate	0.002-0.059

1221

1222

1223

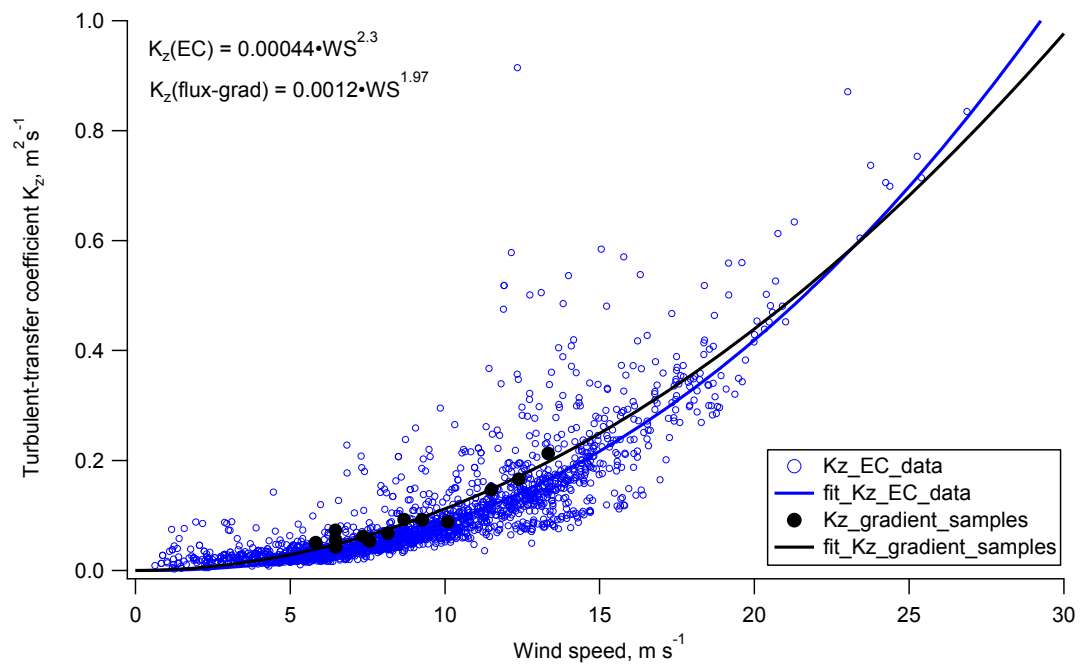
1224 Table 3. Uncertainty of the fitted parameters (\pm one standard deviation) of
1225 derived parameterisations in Figures 7-8.

Parameterisation	Linear coefficient	Power coefficient
Sea salt vs U_{10} $F_{SS}=0.0011U_{10}^{3.15}$	0.0011 ± 0.0014	3.15 ± 0.55
Sea spray vs U_{10} $F_{sea\ spray}=0.0007U_{10}^{3.4}$	0.0007 ± 0.001	3.4 ± 0.6
WIOM vs U_{10} $F_{WIOM}=-0.73+0.10U_{10}$	0.10 ± 0.03	Intercept -0.73 ± 0.28
WSOM vs U_{10} $F_{WSOM}=-0.0013U_{10}^{2.2}$	-0.0013 ± 0.0023	2.2 ± 0.73

1226

1227

1228



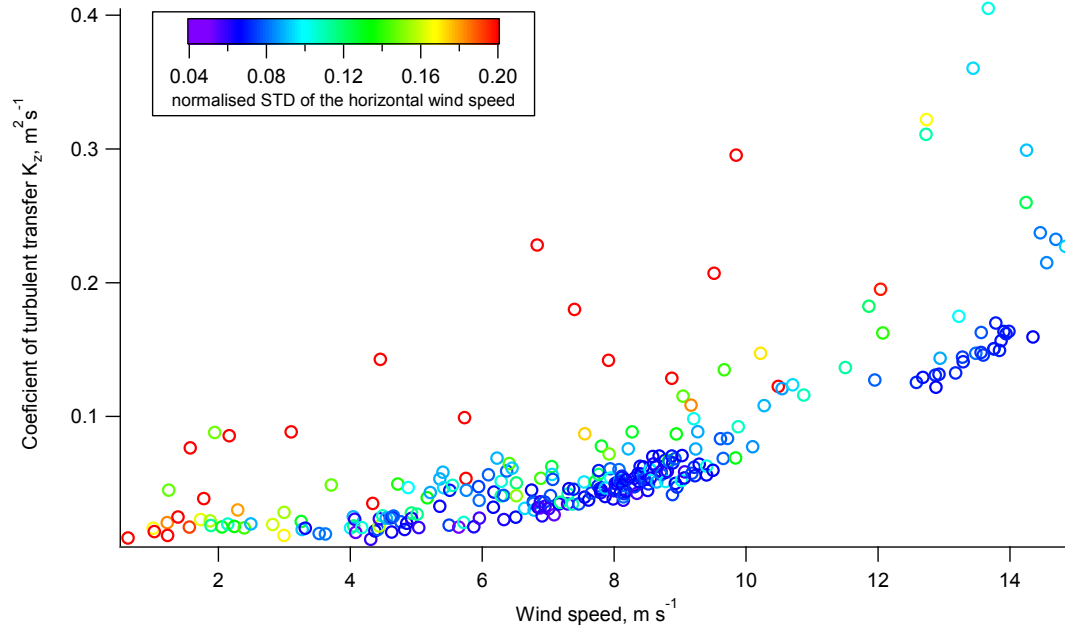
1229

1230

1231 Figure 1. A relationship between the coefficient of turbulent-transfer K_z and the
1232 horizontal wind speed in clean marine air over the whole sampling period. 30
1233 min data from eddy covariance system (blue open circles) and averaged eddy
1234 covariance data for the duration of gradient samples (black circles) were both
1235 fitted by power law relationship.

1236

1237

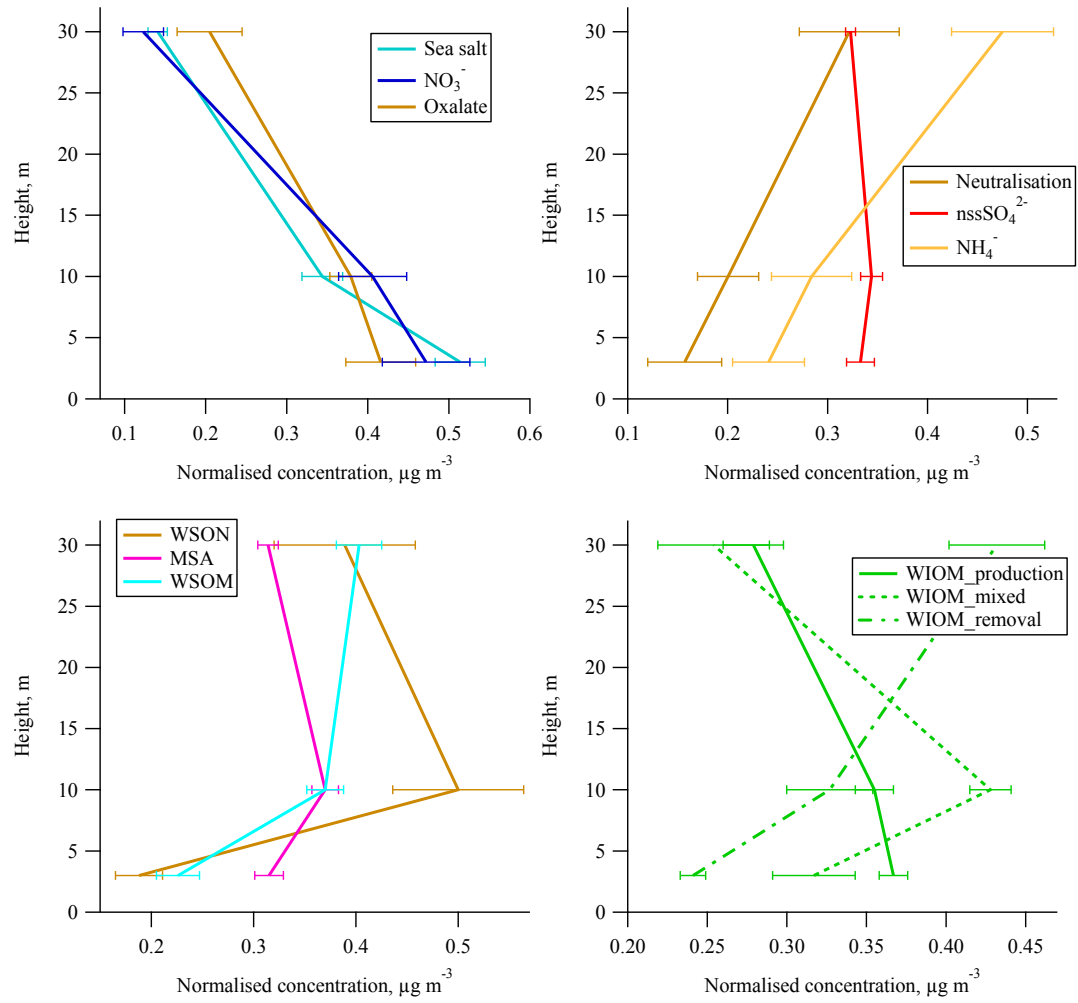


1238

1239

1240 Figure 2. A dependence of the coefficient of turbulent-transfer K_z on the
1241 horizontal wind speed and normalised standard deviation of horizontal wind
1242 speed during April 2008 (a randomly chosen subset of data).

1243



1244

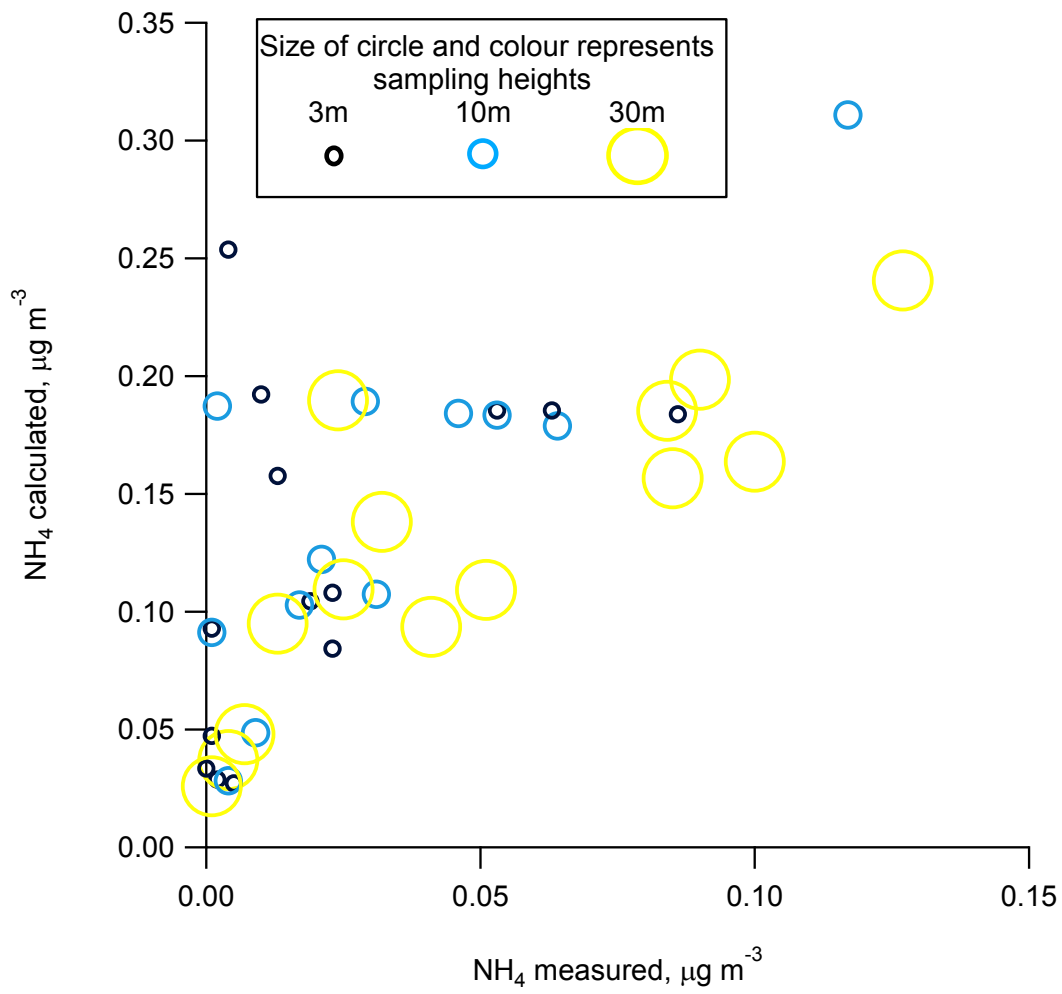
1245

1246 Figure 3. The gradient profiles of chemical species studied: species resembling
 1247 primary production (top left); inorganic species resembling secondary production
 1248 (top right); organic secondary species (bottom left) and water insoluble organic
 1249 matter split into production, removal and mixed profiles (bottom right).

1250

1251

1252



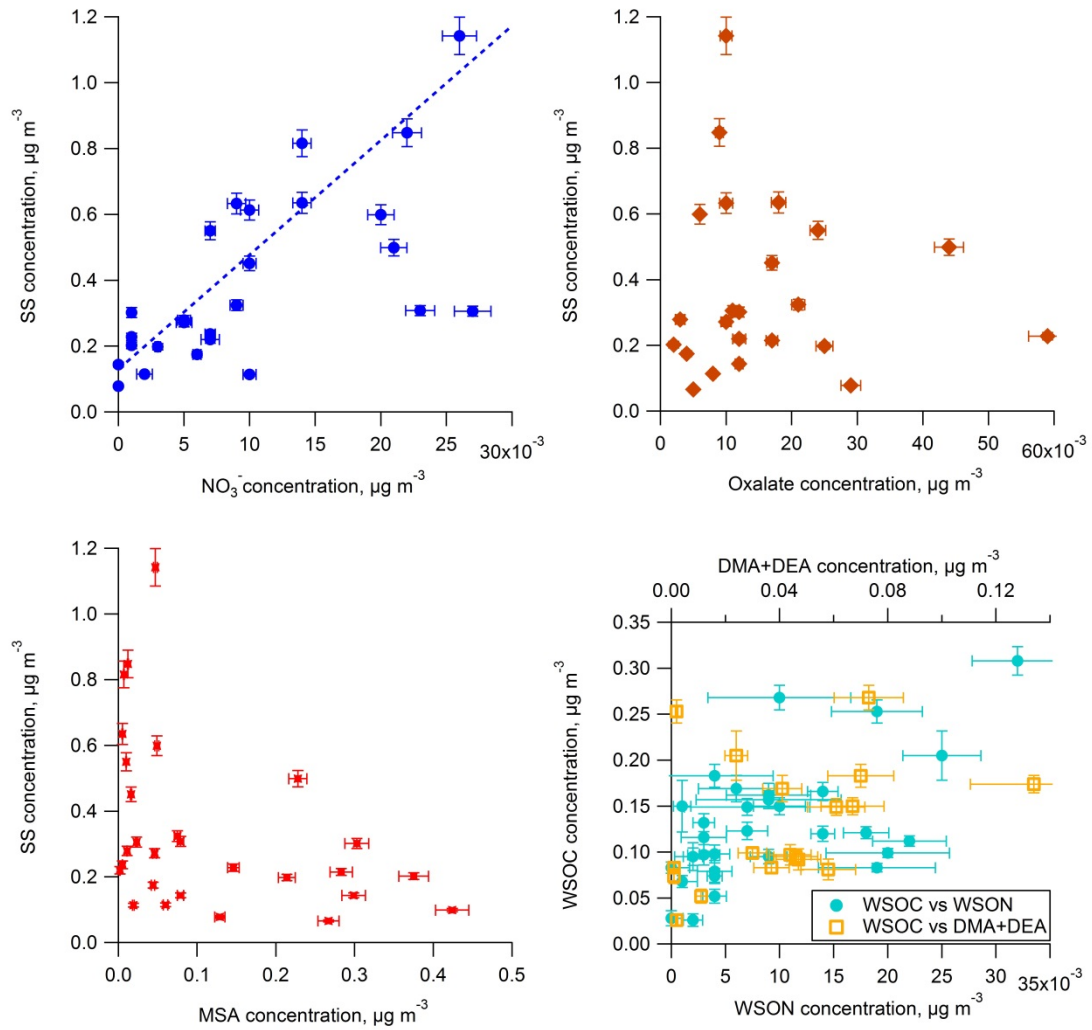
1253

1254

1255 Figure 4. A scatter plot of sulphate neutralisation by ammonium with respect to
1256 sampling height.

1257

1258

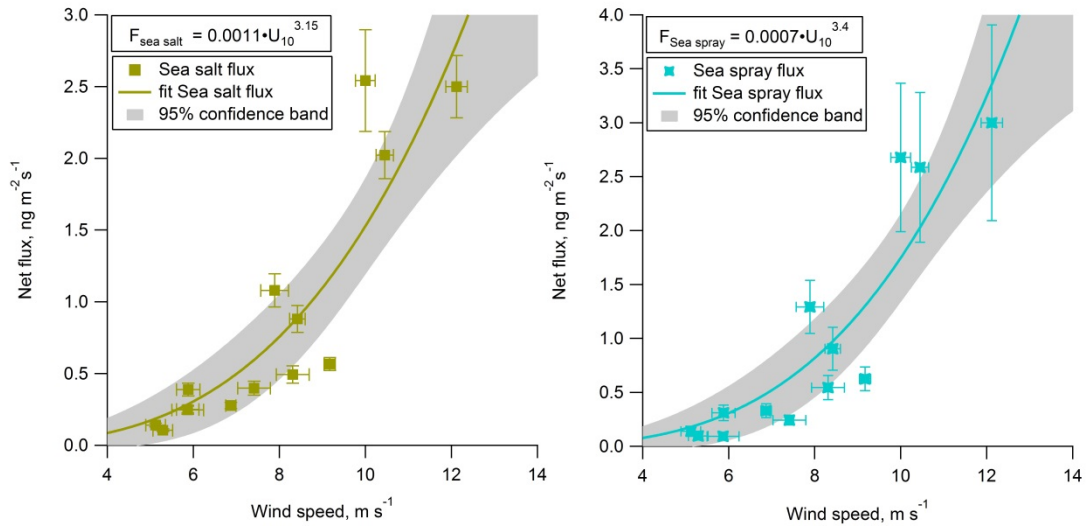


1259

1260

1261 Figure 5. Plots of sea salt and secondary species which resembled primary
 1262 production concentration pattern: SS vs NO_3^- (top left); SS vs Oxalate (top right);
 1263 SS vs MSA (bottom left) and WSOC vs WSON (also plotted as the sum of
 1264 dimethylamine and diethylamine)(bottom right). Note, that WSOC and WSON
 1265 concentration are presented as μg of carbon or nitrogen mass, respectively, while
 1266 all other species reported in absolute species concentrations.

1267



1268

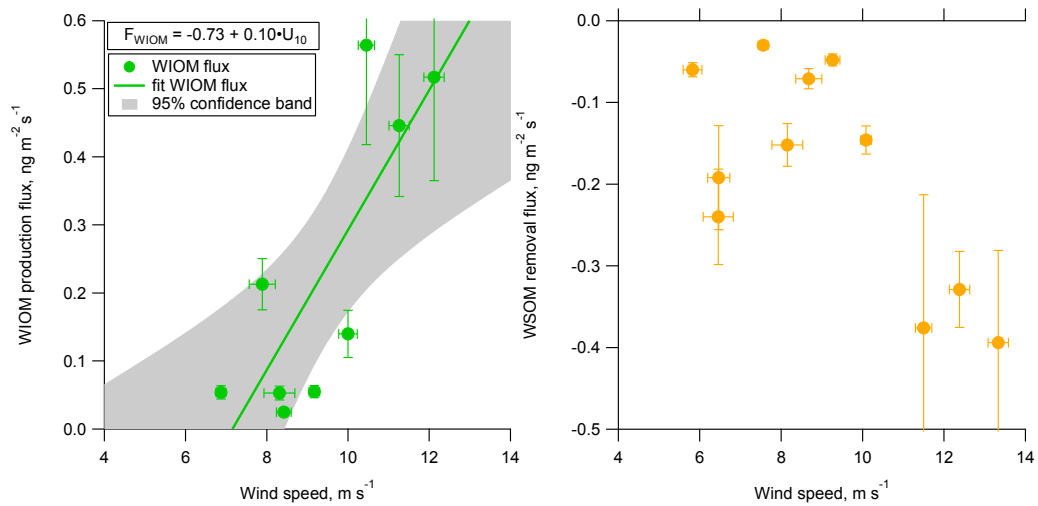
1269

1270 Figure 6. Sea salt and sea spray net production flux versus wind speed.

1271 Individual uncertainties of the flux and wind speed marked with caps while the

1272 grey area denotes 95% confidence bands of the fitted parameterisations.

1273



1274

1275

1276 Figure 7. Water insoluble organic matter net production flux versus wind speed

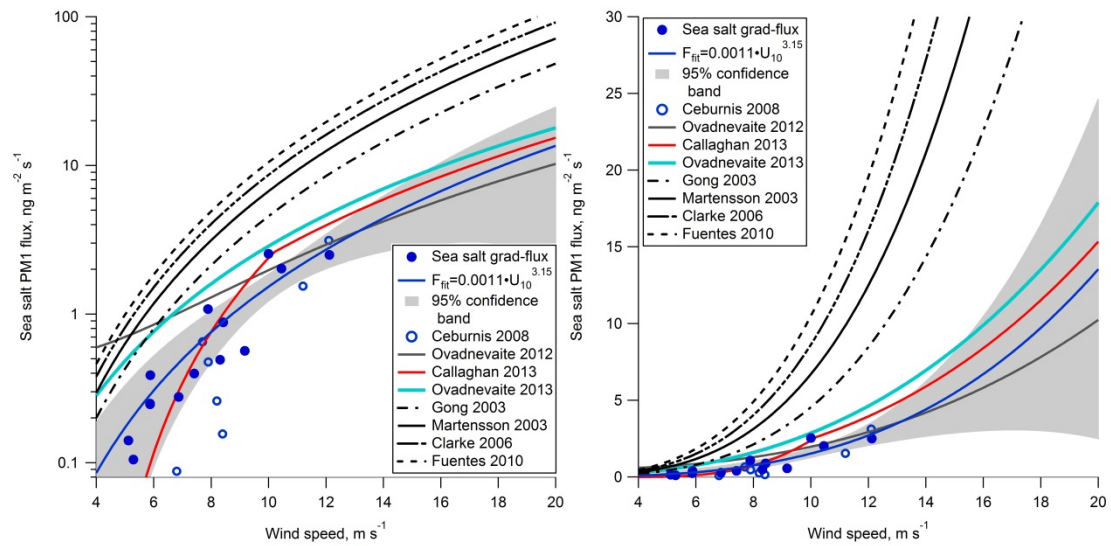
1277 (left) and the dependence of the WSOM removal rate on wind speed (right).

1278 Individual uncertainties of the flux and wind speed marked with caps while the

1279 grey area denotes 95% confidence bands of the fitted parameterisations. WSOM

1280 relationship was not parameterised due to large uncertainties.

1281



1282

1283

1284 Figure 8. A comparison of the most often used and recently developed sea spray

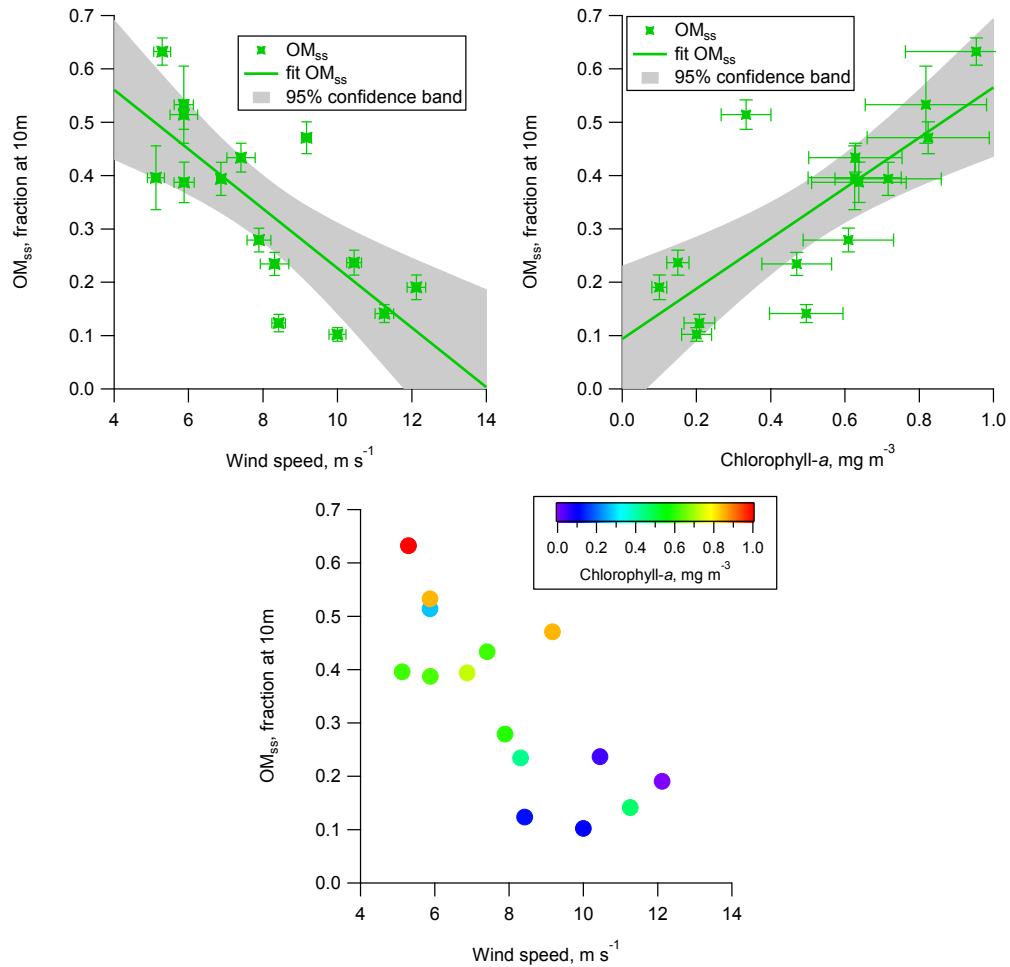
1285 and wind speed parameterisations in log scale (left) and linear scale (right). The

1286 grey area denotes the 95% confidence bands of the flux-gradient fitted

1287 relationship.

1288

1289



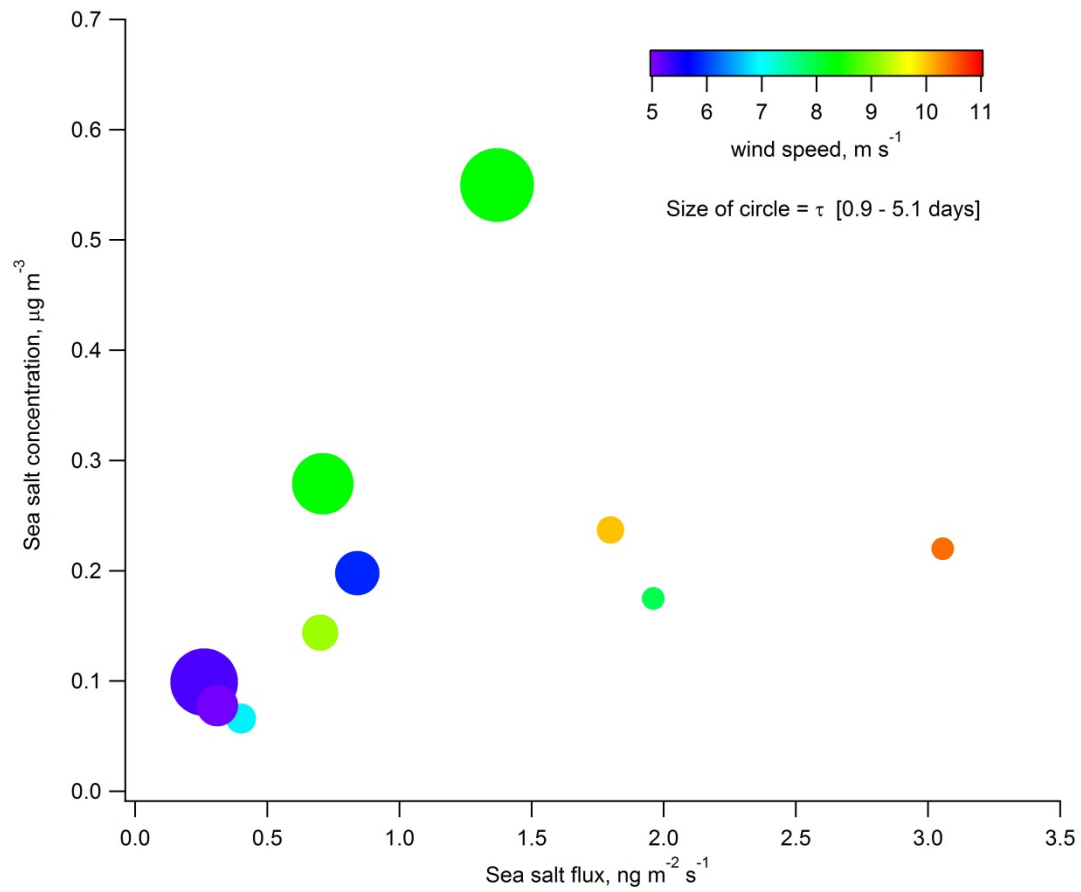
1290

1291

1292 Figure 9. Effect of wind speed and chlorophyll-a concentration on the fractional
 1293 contribution of organic matter (OM_{ss}): OM_{ss} vs WS (top left); OM_{ss} vs
 1294 chlorophyll-a (top right) and OM_{ss} vs WS coloured by chlorophyll-a (bottom).
 1295 Individual uncertainties of the flux and wind speed marked with caps while the
 1296 grey area denotes 95% confidence bands of the fitted parameterisation.

1297

1298



1299

1300

1301 Figure 10. A relationship between sea salt absolute concentration (y-axis), sea
 1302 salt flux (x-axis), wind speed (colour) and boundary layer filling time (marker
 1303 size).

1304

1305